Micromachines **2011**, *2*, 17-48; doi:10.3390/mi2010017

OPEN ACCESS

micromachines

ISSN 2072-666X

www.mdpi.com/journal/micromachines

Review

Self-Assembly in Micro- and Nanofluidic Devices: A Review of Recent Efforts

Hwa Seng Khoo [1], Cheng Lin [2], Shih-Hao Huang [3] and Fan-Gang Tseng [2,4,*]

[1] Institut de Science et d'Ingénierie Supramoléculaires (ISIS), Université de Strasbourg, CNRS UMR 7006, No. 8, allée Gaspard Monge, 67083 Strasbourg Cedex, France; E-Mail: hskhoo@unistra.fr

[2] Department of Engineering and System Science, National Tsing Hua University, No. 101, Sec. 2, Kuang-Fu Rd., Hsinchu 30013, Taiwan; E-Mail: chenglin@mx.nthu.edu.tw

[3] Department of Mechanical and Mechatronic Engineering, National Taiwan Ocean University, No. 2, Pei-Ning Rd., Keelung 20224, Taiwan; E-Mail: shihhao@mail.ntou.edu.tw

[4] Division of Mechanics, Research Center for Applied Sciences, Academia Sinica, No. 128, Academia Road, Sec. 2, Nankang, Taipei 115, Taiwan

* Author to whom correspondence should be addressed; E-Mail: fangang@ess.nthu.edu.tw; Tel.: +886-3-574-2663; Fax: +886-3-572-0274.

Received: 1 December 2010; in revised form: 18 January 2011 / Accepted: 25 January 2011 / Published: 11 February 2011

Abstract: Self-assembly in micro- and nanofluidic devices has been the focus of much attention in recent years. This is not only due to their advantages of self-assembling with fine temporal and spatial control in addition to continuous processing that is not easily accessible in conventional batch procedures, but they have evolved to become indispensable tools to localize and assimilate micro- and nanocomponents into numerous applications, such as bioelectronics, drug delivery, photonics, novel microelectronic architectures, building blocks for tissue engineering and metamaterials, and nanomedicine. This review aims to focus on the most recent advancements and characteristic investigations on the self-assembly of micro- and nanoscopic objects in micro- and nanofluidic devices. Emphasis is placed on the salient aspects of this technology in terms of the types of micro- and nanomaterials being assembled, the principles and methodologies, as well as their novel applications.

Keywords: self-assembly; micro- and nanofluidic; building block

---

1. Introduction

The focus of self-assembly is gradually shifting from fundamental studies on the emergence of life in nature to the synthesis and final assembly of individual micro- and nanocomponents into larger systems and nanostructured materials. The scope of molecular self-assembly from nature such as proteins [1] and nanobiocomposites [2] has been expanded to include man-made materials which have forms such as nanoscopic spheres [3], rods [4], ellipsoids [5], core/shell [6], and nanocages [7]. They can be produced using various types of materials such as metals [6], semiconductors [8], oxides [9], and polymers [10]. Indeed, because of the emergence of new materials, especially those with potential for use in microelectronic, photonic, and biomedical applications, interest in the applications of self-assembly to components larger than molecules have grown dramatically. At a larger scale, self-assembly has been employed to produce microcontainers [11], janus/ternary microparticles of varied packing and surface characteristics [12], large scale crystalline nanoarrays [13], and liposomes [14].

The self-assembly in which these organic and inorganic micro- and nanocomponents interact with one another or with the substrate and organize in two and three dimensions in purposeful ways are predominantly conducted based on bulk techniques. The technical limitations associated with such conventional methods constitute a significant impediment to the realization of many of the aforementioned applications. These limitations include sample size distributions that are polydisperse, irreproducibility from batch to batch, and difficulties in implementing high throughput production, optimization, and screening in batch.

Recent advances in rapid prototyping [15] and soft lithography [16], coupled with mature semiconductor fabrication technology, have brought the field of micro- and nanofluidics to the forefront of their preparations. Micro- and nanofluidic technology is arguably the most promising candidate to overcome the bottleneck of bulk techniques as it enables a range of fundamental features to accompany system miniaturization such as high spatial and temporal resolution, high throughput, ease of chemical and biological micro- and nanopatterning, reduced reagent consumption, high resolution and sensitivity, low cost, well-controlled supply of reagents due to laminar flow, dominant surface tension effect, and potential for sensor and actuator integration. There are several outstanding examples of successful applications of self-assembly in micro- and nanofluidic devices: from material synthesis of plasmonic nanomaterials [17], molecular separation of DNA based on self-patterning of crystalline nanoarray [13], to preparation of temperature sensitive liposome-hydrogel hybrid nanoparticles for targeted delivery [14].

Although several excellent reviews of independent topics on self-assembly [18-21] and micro- and nanofluidics [22,23] have been published, a focus on the self-assembly in micro- and nanofluidic devices is rare. Therefore, this review article aims to present, through selected examples (mostly from 2008 onwards), recent developments in micro- and nanofluidic assisted self-assembly. First, we address the device fabrication, common principles and methodologies of micro- and nanofluidic assisted self-assembly with the types of forces and materials involved. Next, we present a list of selected examples on the use of micro- and nanofluidic assisted self-assembly for a range of micro- and nanoscopic organic and inorganic materials. The readers can then easily choose the intended methods based on the size and types of materials they want to assemble. The principles and

methodologies as well as their novel applications will be emphasized for each example. Finally, the perspectives will be given. We will not provide comprehensive review of all available studies on this topic but only focus on the most recent and characteristic investigations. Overall, it is our hope that this review will provide the readers with the necessary tools to navigate within the large pool of current publications on this topic and to choose their intended methods easily for their applications.

2. Self-Assembly in Micro- and Nanofluidic Devices

In this section, we survey and categorize present strategies used to coordinate the structure and organization of discrete micro- and nanoobjects in micro- and nanofluidic devices. The device fabrication is commented on first, followed by the description of two major methodologies being employed, namely free flow and hydrodynamic coflowing self-assembly, and other interesting new methods such as railed microfluidics and droplet based electrowetting and the forces involved.

2.1. Device Fabrication

The process of self-assembly is conducted in the micro- or nanofluidic devices and the devices are most commonly made of polymers, in particular poly(dimethylsiloxane) (PDMS), silicon, and glass. The fabrication of the devices follows the standard soft lithography protocol described in detail elsewhere [24]. Basically, the method involves standard photolithography steps with negative photoresist, followed by the silicon elastomer casting onto the cured negative photoresist mold and subsequent curing process. After the curing, the PDMS is peeled off and bonded to a glass to seal the channels. These devices are easy to fabricate at low cost and often make excellent prototypes.

2.2. Methodology

2.2.1. Free-Flow Self-Assembly

Free-flow self-assembly is a promising way for large scale, parallel fabrication of devices made up of many small components. Typically, this type of self-assembly process is conducted in bulk solution but it can be readily extended into micro- and nanofluidic devices. In brief, the micro- and nanoscopic objects are normally self-assembled at lithographically [25] or chemically [26] defined precise locations on a chip with the assistance of capillary interactions with the objects at the three-phase vapor-suspension-substrate contact line during controlled solvent evaporation [25], magnetic and electrostatic interaction [26], hydrodynamic flow [27], and gravity [28]. Self-assembly of these objects can also be promoted autonomously even without the predetermined patterned locations. These self-assembly methods use mainly the forces such as fluidic force [29], molecular force [30], surface force [31], and even the use of cell traction force [32] to form two and three dimensional micro- and nanostructures. Such self-assembly methods are often massively parallel and therefore faster and cheaper than conventional serial pick-and-place assembly. When a microfluidic device is coupled with the free-flow self-assembly method, a range of three dimensional micro- and nanoparticle crystalline structures can be formed [13,33]. A variety of interesting applications to assemble a range of organic and inorganic micro- and nanomaterials has been demonstrated including the construction of two dimensional devices such as micropump (superparamagnetic microparticles) [34], on-board electronic

packaging (semiconductor microdevice) [35], nanoelectronics (carbon nanotubes) [36], tunable plasmonic waveguides (gold and silver nanoparticles) [25] and three dimensional devices such as anticancer drug tester (multicellular spheroids) [27], drug delivery microcontainer (metallic plates) [37], molecular sieving system (silica nanoparticles) [13], *etc.*

2.2.2. Hydrodynamic Coflowing Self-Assembly (Droplet Flow, Plug Flow, and Laminar Flow)

Continuous hydrodynamic coflowing-based microfluidic self-assembly methods provide another alternative, promising superior control over reaction conditions while operating at steady-state, thus simultaneously ensuring reproducibility. Scaling to higher production rates is straightforward in principle and involves parallelization of multiple reactor units. Interestingly, this hydrodynamic coflowing method can produce three types of flows, namely droplet, plug, and laminar flows [38]. The types of flows depend on two parameters: capillary number (*Ca*) and water fraction (wf). The capillary number is a measure of viscous stress relative to interfacial tension stresses, $Ca = U\mu/\gamma$, where U is the flow velocity, μ is the dynamic viscosity, and γ is the surface tension at the interface between the aqueous solution and the carrier fluid. Water fraction (wf) is defined as the combined flow rate of the aqueous phase to the total flow rate of the carrier fluid and the aqueous phase. Normally, a low *Ca* (surface tension dominant) will tend to generate plugs, a medium *Ca* (shear force becomes larger) will tend to produce droplets, while a high *Ca* (shear force dominant) induces a laminar flow and the range of *Ca* describing each regime varies as water fraction (wf) changes. A variety of interesting applications to assemble a range of organic and inorganic micro- and nanomaterials inside the droplets, the plugs or along the interface of the laminar flow has been demonstrated including spherical janus for photonic crystals (polymeric microparticles) [12], liposomes for cell membrane study (polymeric lipid bilayer) [39], scaffolds for cell culture (microbubbles) [40], multicomponent nanoparticles for therapy and diagnosis (lipid-polymer and lipid-quantum dot nanoparticles) [41], *etc.*

2.2.3. Other Methods

There are other new micro- and nanofluidic methods to assist the self-assembly of micro- and nanoscopic objects such as railed microfluidic self-assembly [42] and droplet based electrowetting [43]. These methods will be described and discussed in the following sections.

3. Self-Assembly of Microscopic Objects

In this section, we present a list of selected examples on the use of micro- and nanofluidic assisted self-assembly for a range of microscopic organic and inorganic materials. The size and types of materials, the principles and methodologies as well as their novel applications will be emphasized for each example.

3.1. Organic

3.1.1. Spherical Janus and Ternary Polymeric Microparticles

Janus particles have long been fascinating objects in the study of self-assembly, in stabilization or emulsions, and as dual-functionalized optical, electronics, and sensor devices [44,45]. They are

produced by hydrodynamic techniques that commonly employs breakup of a liquid thread of two parallel coflowing streams of monomers or polymer solutions with no control of the internal structure or of the surface composition of the microbeads. In addition, the counterpart liquids are miscible and the interface between the phases is not sharp. Nie *et al.* successfully employed continuous microfluidic synthesis of highly monodisperse janus and ternary polymer particles with sharp interface in the size range from 40 to 100 μm with precise control of their structures and their structure-dependent assembly in clusters [12]. The schematic illustration of the device is shown in Figure 1. The morphology of janus and ternary droplets was governed by the combination of hydrodynamic and thermodynamic factors and highly depended on the values of interfacial energies between the liquids. Immiscible janus and ternary droplets with different volume fractions of different phases were solidified by *in situ* photoinitiated free-radical polymerization. Fast polymerization of multiphase droplets guaranteed one to trap the structures of droplets in the solid state with sharp interface. With their amphiphilic nature, the polymerized microdroplets underwent self-assembly at the water-oil interface. The selective functionalizations of biomolecules on the surfaces of the polymer janus particles were also conducted to promote bioconjugation among the particles.

This technology has been further developed to produce more complex multifunctional janus particles. Yuet *et al.* recently reported the use of the same hydrodynamic technique for the synthesis of a multifunctional janus hydrogel particle with anisotropic superparamagnetic properties and chemical composition for bottom-up assembly of hydrogel superstructures [46]. By exposing the janus particles to a uniform rotating or in-plane/out-of-plane magnetic field, the janus particles reorient themselves or self-assemble into chainlike or meshlike superstructures, the complexity of which can be simply modulated by particle density and composition. The janus particles were also selectively copolymerized with biological payloads such as DNA probes to capture complementary targets in the solution. The field-driven assembly of large-scale and novel tunable anisotropic configurations of janus particles undoubtedly can be potentially used in several exciting areas of research such as photonic crystals, novel microelectronic architecture, sensing, and building blocks for tissue engineering and metamaterials.

Figure 1. A microfluidic system for the formation of ternary polymer microparticles from immiscible monomers M1 and M2, emulsified in an aqueous solution of sodium dodecylsulfate (W). The droplets are irradiated with UV light in the downstream channel. (Reprinted with permission from [12]. Copyright 2006 American Chemical Society).

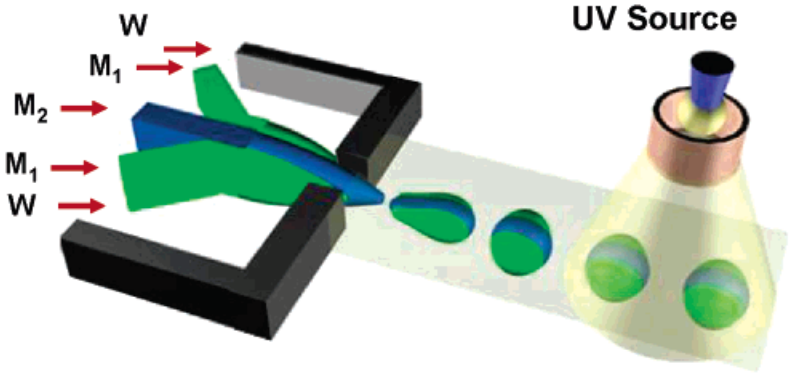

3.1.2. Nonspherical Polymeric Microparticles

While spherical polymeric particles are ubiquitous and have a wide range of applications ranging from drug delivery to paints and catalysis, the synthesis and self-assembly of amphiphilic, nonspherical, polymeric microparticles offer several unique advantages relative to their spherical counterparts such as their ability to assemble into a wide range of crystal structure unavailable to spheres [47] and their anisotropy-driven response to interfacial forces and external fields, which could lead to a variety of technologically important applications. Dendukuri *et al*. developed a microfabricated method named continuous flow lithography by synthesizing the wedge-shaped particles bearing segregated hydrophilic and hydrophobic sections in a microchannel by polymerizing across laminar coflowing streams of hydrophilic and hydrophobic polymers [48]. The schematic illustration of the device is shown in Figure 2. Using continuous flow lithography, mask-defined shapes were polymerized using short pulses of UV light, and the extent of each chemistry can be tuned simply by moving the microscope stage or by altering the width of the streams when more than two streams present. The length scale of the amphiphilic particles synthesized could possibly be pushed down to 10 μm. The amphiphilic particles were allowed to self-assemble in water to form micelle-like structures or at water-oil interfaces to align to the oil-water interface to minimize their surface energy. With careful design of the synthesis, the particles could serve as bar-coded particles with multiple chemistries that find applications in diagnostic and medicine where the detection of multiple analyte species simultaneously is of great importance.

Figure 2. Schematic depicting the formation of biphasic particles. Mask-defined wedge shapes are polymerized, five at a time, across two parallel coflowing streams containing hydrophilic and hydrophobic chemistries using continuous flow lithography. (Reprinted with permission from [48]. Copyright 2007 American Chemical Society).

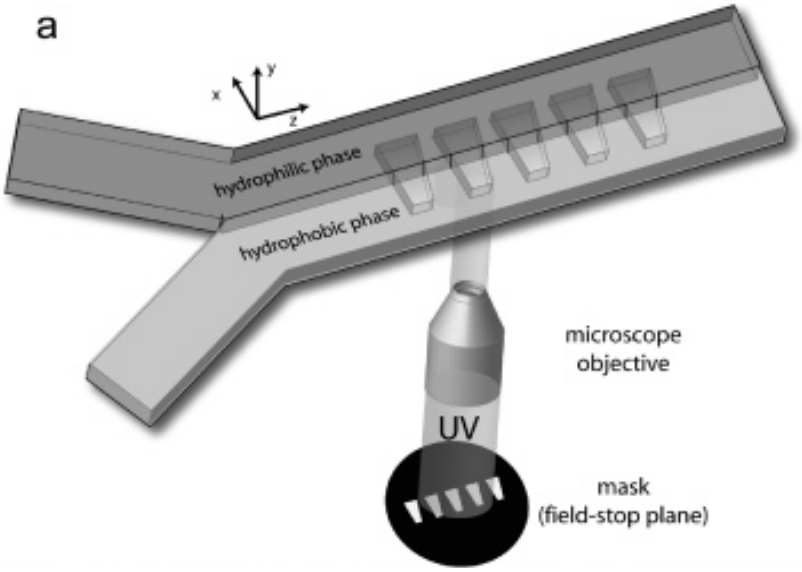

3.1.3. Complex System of Polymeric Microstructures

The railed microfluidic process [42,49-52] is an innovative technique to guide the movement of *in situ* photopolymerized microstructures as shown in Figure 3. Rail-based guiding was applied to

self-assembly in order to overcome many limitations of conventional free-flow self-assembly. Briefly, microparts are sent to the assembly site at the end of the rail by microtrain. At the end of the rail, the microtrains are blocked to initiate the assembly process. The concept of railed microfluidics can be thought of as a microscale version of a monorail where a train follows the monorail due to the matching shapes of the train body and the rail [42]. This shape matching concept was implemented in microfluidic channels by uniquely combining a grooved microfluidic channel [49] with the technique of the optofluidic maskless lithography [50]. A groove ("rail") was formed on the top surface of the channel using two-step mold fabrication by the standard soft lithography. The groove functions as a guide rail track inside the microfluidic channel. After the channel was filled with UV-curable oligomer solution, a polymeric microstructure with a fin ("microtrain") was created using *in situ* photopolymerization via optofluidic maskless lithography.

The real benefit of railed microfluidics over the conventional fluidic self-assembly lies in its capability to assemble complex systems made up of a large number of different parts with different materials, or heterogeneous assembly in a deterministic way. For example, railed microfluidics can easily be applied to assemble living cells for biomedical tissue engineering. Using railed microfluidics, many different types of cells with an exact specified configuration can be assembled. The patterning of many different cells in a hydrogel substrate is an important task in tissue engineering and in cell-based biochips. Kwon *et al.* demonstrated the rail-based heterogeneous assembly to form a 3 × 3 microscale hydrogel matrix with two different living cells, HeLa transfected with green fluorescent protein and HEK293 transfected with red fluorescent protein [42,51]. This heterogeneous matrix was formed in single-step lithography, precluding the need for multiple alignment steps. Besides, the rail-guided assembly technique also has applicability in industrial processes for the integrated chip packaging to locate and assemble externally fabricated silicon chips, such as radio frequency identification and light-emitting devices smaller than 200 μm [52,53].

Figure 3. (**a**) Schematic diagram of a railed microfluidic channel. (**b**) Cross-section of the poly(dimethylsiloxane) (PDMS) railed microfluidic channel and a finned microtrain cut at a–a' from a. (**c**) Fabricated microtrain. Left: the top view of the microtrain in a differential interference contrast image. Right: a corresponding scanning electron microscope image. (Reprinted by permission from Macmillan Publishers Ltd: Nature Materials [42]. Copyright 2008).

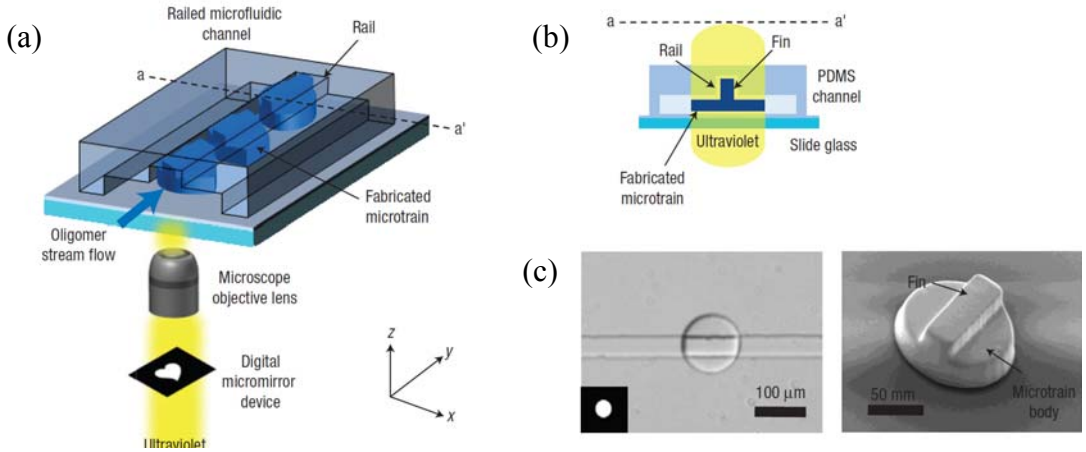

3.1.4. Three Dimensional Parylene Microstructures

A number of methods have been developed to produce three dimensional microstructures by folding of connected two dimensional plates through physical interaction forces involved during self-assembly in micro- and nanofluidics such as electrostatic forces, magnetic forces, capillary force, *etc.* [18]. However, these methods still need additional driving forces to produce three dimensional microstructures by folding of connected two dimensional plates during self-assembly. Takeuchi *et al.* proposed a new strategy for fabricating three dimensional microstructures by using power of the cells as shown in Figure 4 [32,54]. The cells can be powerful tools since they have several self-forces such as locomotion and traction forces for their migration. They used cell traction forces to produce three dimensional microstructures. Briefly, they seeded cells onto the parylene microplates on a glass substrate; the cells were adhered and stretched onto the plates. Immediately after detaching the plates from the substrate, the plates were lifted and folded up into three dimensional structures due to the traction forces caused by stretched cells between two plates. Advantages of using the parylene as a supporting material are due to the facts that it can be patterned by standard photolithography and peeled off from the substrate easily [32]; as well as its transparency to observe assembly of the parylene plates by microscopy. Furthermore, unlike other elastic sheets, the parylene does not wrinkle by the adhered cells. After detaching the plates from a glass substrate, the parylene plates are self-folded by the cells and form the three dimensional structures. During the folding, other type of cells are also encapsulated into the structures for heterotypic three dimensional co-culture. They also successfully demonstrated the feasibility to produce three dimensional microstructures in various shapes such as cube, tetrahedron and dodecahedron using the 3T3 cells. They also achieved more complicated structures by assembling several three dimensional structures to produce the cell balls with two different types of the cells: 3T3 and HepG2 (hepatocyte cell), which is useful for the cell-cell interaction analysis.

Figure 4. Conceptual illustration of assembly of micro-sized three dimensional structure by cell traction forces. A dodecahedron (cell ball) is folded by the cells. During the folding, other types of cells are also encapsulated into the cell ball for heterotypic three dimensional co-culture [54].

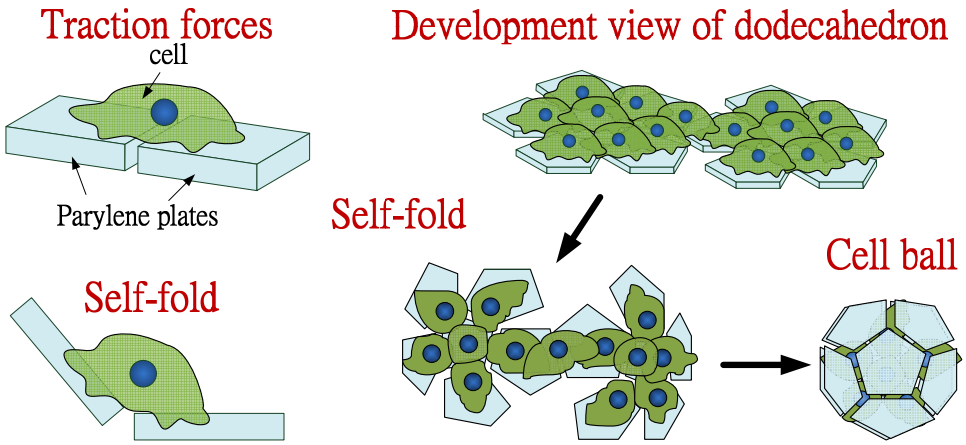

3.1.5. Lipid Vesicles

Lipid vesicles are widely used as functional delivery vehicles in pharmaceuticals and cosmetics or as biochemical reactors that respond to various environmental stimuli [55]. Besides, phospholipid vesicles are also attractive materials to mimic the complex cell biomembrane, which is required to study and control membrane behavior and transport through incorporated membrane proteins [56]. Cell-sized vesicles offer desirable spatial and temporal scales to mimic the kinetic behavior of living cells [57]. To efficiently use vesicles for these applications, the vesicle production methods are required to simultaneously control unilamellarity, encapsulation efficiency, and vesicle size, which should be uniform and comparable to cell size. Despite a variety of methods previously developed to form lipid vesicles, such as reverse emulsion [57], jetting [58], and double emulsion [59], none of them has been able to produce the cell-sized unilamellar vesicles with high uniformity in size and high encapsulation efficiency. Recently, Takeuchi *et al.* proposed a new microfluidic approach for continuous generation of monodisperse cell-sized unilamellar vesicles from a microfluidic T junction as shown in Figure 5 [39]. They began to reconstitute a lipid film in the junction by sequentially infusing water, oil, and water into the device. In this film, amphiphilic lipid molecules self-assemble into two monolayers at both water-oil interfaces. Then, the cross flow at the T junction continuously thins, shears, and squeezes the membrane, and this membrane eventually releases multiple vesicles encapsulating uniform water droplets. They also demonstrated efficient encapsulation of concentrated compounds inside monodisperse vesicles and molecular transport through the functional pore proteins incorporated in the unilamellar membrane, as well as a cell-free gene expression system to build a cell-like reactor toward developing artificial cells.

Figure 5. A microfluidic technique using a continuous fluid stream to generate monodisperse unilamellar phospholipid vesicles from a single bilayer (Reproduced with permission from [39]. Copyright 2009 Wiley-VCH Verlag GmbH & Co. KGaA).

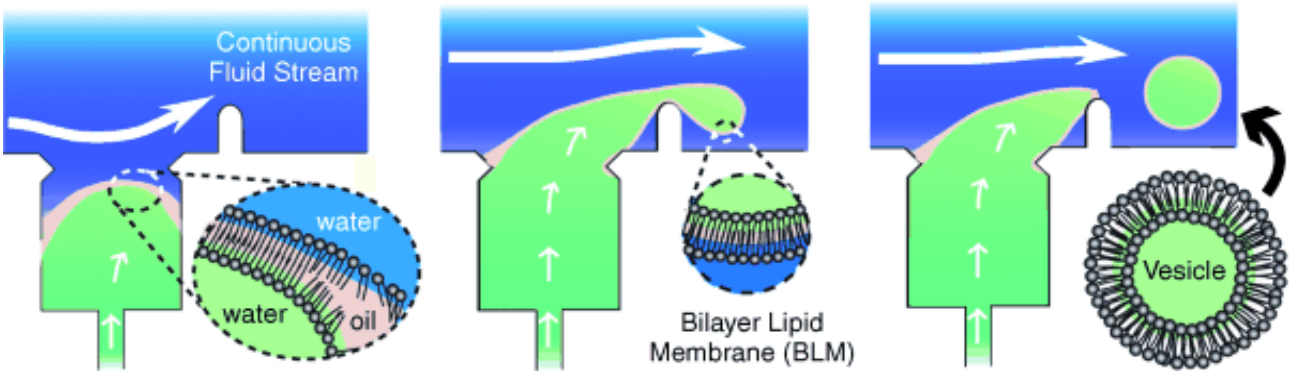

3.1.6. Multicellular Spheroids

Multicellular spheroids have recently received a great deal of attention in cell biology research and have been applied to the evaluation of anticancer drugs [60]. This is because the 3D multicellular aggregates more accurately simulate the cell microenvironment *in vivo* by reproducing nutrient and signal gradients and by removing the effect of unnatural adhesion to artificial surfaces or gels. There are several microfluidic techniques to form tumor spheroids, but most of them lack the ability to

precisely control the number of cells in each spheroid and do not allow testing on the growth platform. Lee *et al.* proposed a new microfluidic approach allowing microfluidic self-assembly of spheroids, formation of uniform spheroid arrays, and characterization of spheroid dynamics all in one platform [27]. Their microfluidic device is based on hydrodynamic trapping of cancer cells in controlled geometries and the formation of spheroids is enhanced by maintaining compact groups of the trapped cells due to continuous perfusion. With this platform, antitumor assays can be conducted immediately after the spheroid formation in the growth platform. This may lead to identification of improved dosage regimes for anticancer drugs in preclinical *in vitro* experiments, saving time and reducing costs. Recently, Negishi *et al.* also proposed a similar PDMS microchamber array to facilitate the self-assembly of multiple neurospheroids, which in turn interconnected via neuronal processes to form a centimeter-sized neurospheroid network [61].

3.2. Inorganic

3.2.1. Silica and Silica Gel Microparticles

The control of two dimensional microparticle assembly from the liquid suspension of microparticles can be achieved in confined geometries by either a receding contact line [62,63] or electrostatic forces [64] where the particles are directed from the suspension to fill the trenches. However, the methods require careful control of the receding speed of the contact line and the contact angle of the meniscus of the fluid with respect to substrates. In addition, the release of particle structure in the confined geometries has not yet been demonstrated, which is crucial in the integration of on-chip particle assemblies with other micro-devices. Recently, Choi *et al.* developed an ultrafast microfluidic method to self-assemble silica microparticles in three dimensions by using simple photolithography and the surface-tension induced capillary action of a microparticle dispersed suspension [33]. Silica and silica gel microparticles were rapidly self-assembled within a thin, long, open micro-channel and self-supported particle-based patterns within the channels were fabricated by dissolving the photoresist. The crystal growth rate of particle assembly was theoretically estimated by combining the model of convective assembly of colloid particles with the open-channel flow model. Due to its compatibility with integrated circuits processes and wide applicability to various types of particles and substrates, this method is potentially useful in various applications such as chromatography and micro-filter in on-chip bioassay, micro-structures on cell chip, and tunable three-dimensional photonic crystals for waveguide and micro-cavity structures.

3.2.2. Para- and Superparamagnetic Microparticles

Self-assembly in micro- and nanofluidic devices can also be conducted based on magnetic field assisted self-assembly of para- and superparamagnetic microparticles. In some occasions, it is applied to the development of microscale mixing and pumping devices. Efficient pumping and mixing are of great importance in microfluidics applications. Since low Reynolds number exists and one encounters hydrodynamics that is conceptually different from the macroscopic turbulence world, novel methods to produce pumping and mixing in the microscale regime are highly sought after. By combining external

magnetic fields and colloidal superparamagnetic particles, actuation microdevices such as a microscale pump can be developed and probably even a nanoscale pump could be envisioned.

Blei *et al.* developed a bulk-field based *in situ* method which allows the fabrication of micropumps from simple colloidal building blocks [34]. Here, the assembly of a few superparamagnetic microparticles into a compact rotating cluster in the presence of a rotating magnetic field was observed in the specially designed microchannel. The rotating external magnetic field induced a torque on the cluster due to the interaction with the magnetic dipoles and cluster formation was irreversible due to van der Waals forces. The size of the resulting micropumps can be adjusted on-spot by applying an additional static vertical magnetic field inducing a repulsive particle interaction. Multiple colloidal pumps were also formed to produce higher pumping rates. This bulk-field approach avoids the need for individual manipulation allowing for both scale down to the true nanoscale regime and the simultaneous assembly and control of highly parallel device networks. Recently, Vilfan *et al.* also demonstrated the realization of an effective pumping device based on the magnetic field mediated self-assembly and manipulation of superparamagnetic microparticles [65]. This artificial celia device mimics a ciliated surface and imitates its motion to generate fluid flow in synchronized tilted conical motion and nonreciprocal manner.

Figure 6. Schematic illustration showing the concept of specific capture from a cell mixture of MCF-7 cells on self-assembled beads micropatterned *in situ* inside a microfluidic channel, followed by subsequent culturing. (Reprinted with permission from [26]. Copyright 2010 American Chemical Society).

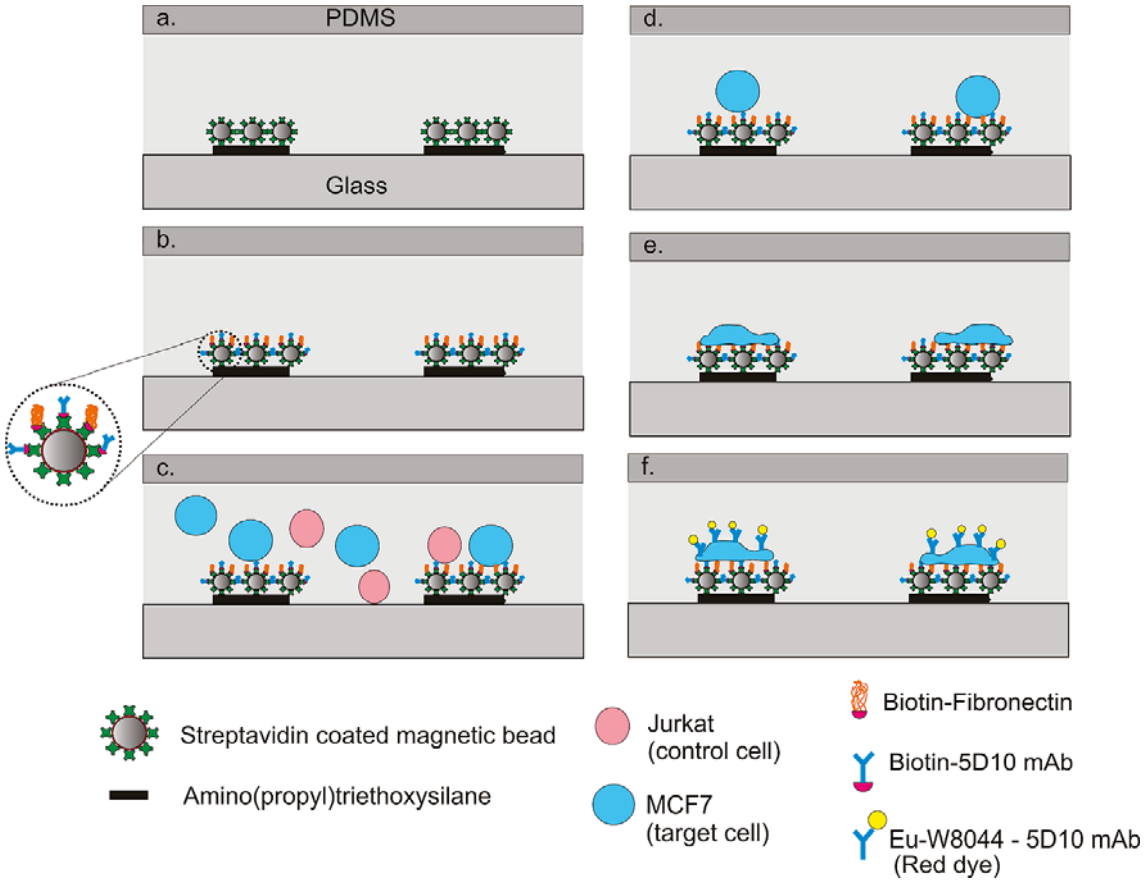

Another application of magnetic field assisted self-assembly of para- and superparamagnetic microparticles is on the label-free target cell arraying. Label-free separation of target cells based on specific physical and chemical interactions between the cell surface and the substrate are interesting methods due to their minimal interference during the subsequent assay tests. In particular, immunoaffinity based cell separation is a very popular choice due to its simplicity and specificity. Recently, Sivagnanam *et al.* developed a separation and subsequent culturing of human breast adenocarcinoma cell line MCF-7 based on magnetic field assisted electrostatic self-assembly method [26]. The schematic illustration of the concept is shown in Figure 6. The rapid self-assembly took place when the negatively charged streptavidin-coated magnetic particles dispersed in the solution were pulled close to the positively charged silane based dot patterns on the microfluidic chip by the external magnetic and attracted to them through electrostatic interactions. These *in situ* microparticles were then grafted with monoclonal antibodies and fibronectin for subsequent immunospecific cell culture and cell adhesion and growth.

3.2.3. Monodisperse Microbubbles

To grow a functional tissue or organ, it is necessary to culture cells in three dimensions. Three dimensional scaffolds which have uniform pore size, shape, and spatial structures are highly sought after so that systematic studies on the architecture influence of the differences in signaling, gene expression, and organization can be conducted and chemical stimuli can be distributed more homogeneously. Chung *et al.* recently demonstrated the use of microfluidics to fabricate tissue engineering scaffolds with uniform pore sizes based on bubble generation and the application of foam as the scaffold [40]. The microfluidic device was composed of two concentric tapered channels, which were made by micropipettes. Nitrogen gas and aqueous alginate solution with surfactants were pumped through the inner and outer channels, respectively. The monodisperse bubbles were than self-assembled into crystalline structures. The crosslinked open-cell form scaffold was formed by adding $CaCl_2$ to crosslink the alginate and subsequent degassing in the water. The chondrocyte cells were successfully proliferated within the new scaffolds.

3.2.4. Monodisperse Microfoams

Continuous flow-based microfluidic synthesis methods have provided interesting and promising routes due to their superior control over reaction conditions while operating at steady state, thus simultaneously ensuring reproducibility. Duraiswamy *et al.* demonstrated that self-assembly of ordered micro-scale foam can be used for robust and reproducible continuous colloidal syntheses of plasmonic nano-structures [17]. The schematic diagram of the device setup is shown in Figure 7. The microscale aqueous-based electrodeless platings of nanometer-scale multicrystalline gold films or islands onto silica nanoparticle surfaces were conducted inside droplet compartments or so-called cells. Nitrogen gas, an aqueous mixture of gold-seeded silica particles in gold-plating solution and aqueous reducing agent solution were delivered continuously to a microfluidic T-shaped junction, where the reagents were dispersed as aqueous cells within a composite foam lattice. The recirculation fluid motion within the cells promoted rapid mixing and homogenization and the mixing patterns within the aqueous foam cells were extremely robust and display little cell-to-cell variation at any given downstream location.

The intense mixing inside the cell did not entail high shear rates which eliminated the problem of irreversible colloidal aggregation. This technology presents a new technological scheme for continuous plasmonic nanoparticle synthesis where multiphase micro-fluidics and colloidal synthesis are bridged.

Figure 7. (**a**) A two-dimensional conceptual schematic of our nanoshell manufacturing method. (**b**) Diagrammatic representation of the experimental setup. (Reprinted with permission from [17]. Copyright 2010 American Chemical Society).

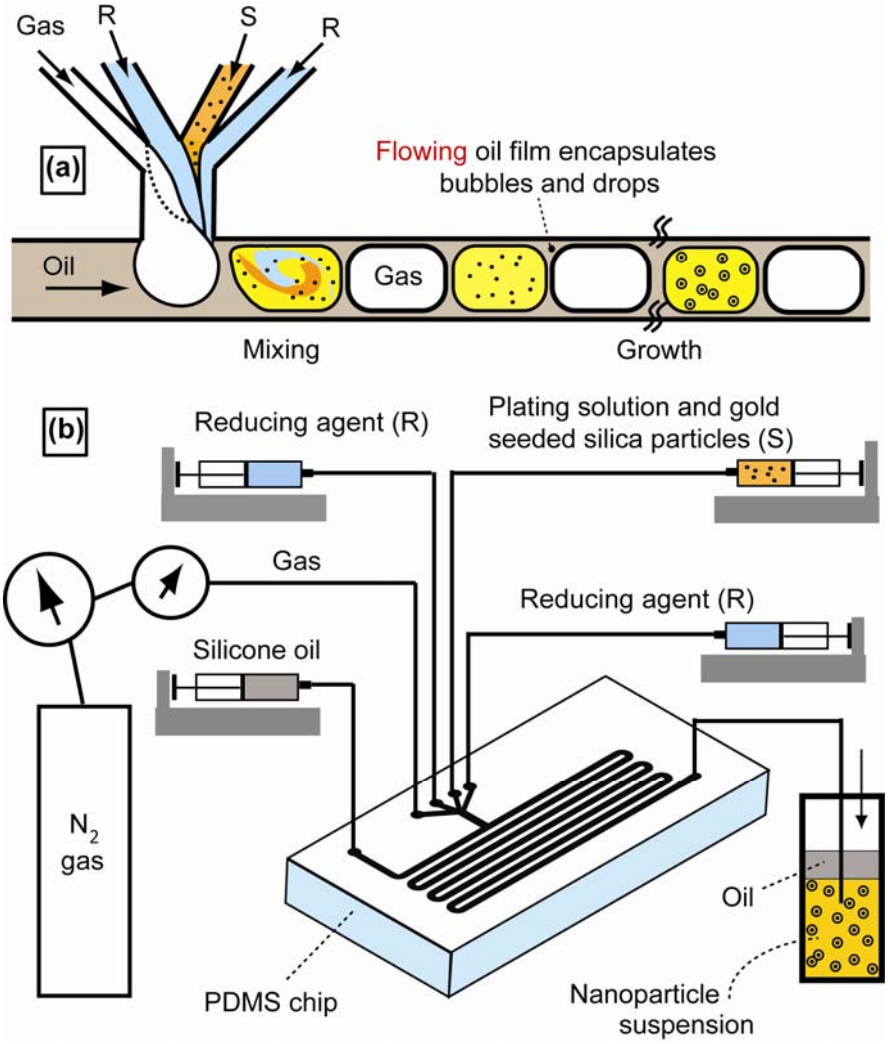

3.2.5. Semiconductor Electronic Packaging

Recent advances of miniaturization and microfluidic technologies bring novel ways of parallel assembly of thousands of microscale electronic components in fluidic phase. Traditional assemblies such as microactuators, microsensors, microcontrollers, and pick-and-place techniques [66,67] are inappropriate for mass production with large numbers of micro parts because of the speed and cost constraints resulted from the serial manipulation and the "sticking problem". Efficient microassembly methods must be parallel approaches to integrate a large number of components in hybrid systems. For the micro- and nanosystems with parts smaller than a millimeter, the acting forces might be primarily due to electrostatic, van der Waals or surface tension. Special manipulators and additional tools were developed to adapt to the micro- and nano-scaled system. In early 2000, Srinivasan *et al.* adopted the

capillary force driven assembly technique to assemble microscopic parts onto desired sites on silicon and quartz substrate [68]. In their technique, the substrate and hydrophobic alkanethiol self assembled monolayer-coated gold were patterned on hydrophilic background. A hydrocarbon lubricant, deposited exclusively on the hydrophobic patterns, attracted and assembled the microscopic parts in water, and it was then cured to physically bond the parts. Xiong *et al.* demonstrated the extension to multiple-batch assembly and bonding of microparts driven by capillary force with treated hydrophobic sites using self-assembled monolayer desorption, electrochemical method, and electroplating in parallel manner and applied the technique to generic parts such as surface mount light emitting diodes [35].

This type of so-called fluidic self-assembly is a promising technique to overcome fundamental limitations with integrating, packaging, and general handling of individual electronic-related components with characteristic lengths significantly smaller than 1 mm. From 2008 onwards, many research groups have studied various fluidic self-assembly systems, which employ various driving forces such as gravity, surface tension [69,70], electrostatic or electromagnetic force and they often require adhesives, liquid solder, shape matching structures or two different liquids [71]. Knuesel and Jacobs developed a process of self-assembling solar panels based on surface tension-directed self-assembly of ultra small dies at the oil/water interface as illustrated in Figure 8. This study introduced a method for self-assembling and electrically connecting small (20–60 μm) semiconductor chiplets at predetermined locations on flexible substrates with high speed (62,500 chips/45 s), accuracy (0.9 micrometer, 0.14°), and yield (>98%). Other fluid self-assembly techniques utilized load-free oxide-oxide direct bonding of self-assembled chips to wafers at room temperature after liquid evaporation when they used a solution of hydrogen fluoride in water as a liquid. This paper suggested that hydrogen fluoride concentration strongly influenced the bonding strength of self-assembled chips to wafers [72]. Arase and Nakagawa used a novel blade-coating technique that takes advantage of capillary force for rectangular-shaped SiO_2 plates of micrometer-size onto selected areas on large-scale substrates [73].

Figure 8. Procedure of surface tension-directed self-assembly at a liquid-solid interface (diagram illustrating the substrate being immersed and withdrawn from a silicone oil /water interface) (Reprinted with permission from [71]. Copyright 2010 Proceedings of the National Academy of Sciences).

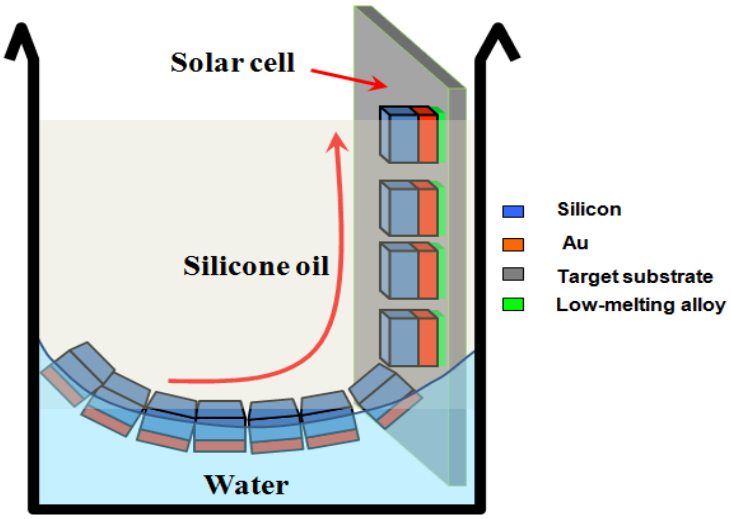

Other researchers [74] performed blowing tests to estimate the maximum adhesion force binding flat parts onto confined lubricant drops. Higher filling ratios and higher precision ratios were obtained for larger microparts (thicker or longer side length) from 350 × 350 μm^2 to 1,000 × 1,000 μm^2 and the success can be explained by higher adhesive force and higher overlap ratio due to higher surface tension and larger adhesive area. Lin *et al.* compared two dimensional numerical results with experiments [75]. The computational model was based on first principle conservation equations and was constructed by the coupling of two phase modeling using volume of fraction, solid structure modeling, and fluid-structure coupling. The authors observed a good match of their two dimensional simulation to experimental data in the case of fluid meniscus aspect ratios larger than 3. The substrate with the binding sites, which was coated with the gold film, was dipped into the solder bath to carry out the solder patterns on the receptor arrays, or the solder droplet was dripped directly onto the receptor binding sites. The parts were put onto an alignment template with the face orientation preserved, and the aligned parts were transferred to a target substrate via the solder capillary force. That pattern was further developed and a tear-drop pattern with an elliptical hole was studied [76]. A 100 % unidirectional assembly yield was achieved with the tested 1,100 μm × 1,100 μm × 440 μm part.

3.2.6. Three Dimensional Metallic Microcontainer

The self-assembly of three dimensional objects on the micro- and nanoscale with any desired patterns based on surface force has been successfully demonstrated [77,78] and is potentially useful if coupled with micro- and nanofluidic applications. Ye *et al.* has successfully combined microfabricated nanoliter scale fluidic devices with wireless technology by fabricating remote-controlled cubic microcontainers for temporal and spatial chemical delivery [37]. The gold-coated, nickel nanoliter containers were fabricated based on a combination of conventional microfabrication and self-assembly [77,78]. To facilitate chemical delivery, the containers were filled with a gel that was soaked in the chemical reagent to be released. Once loaded, a container was guided by the magnetic styles and by heating the metal container with radio-frequency field generated by a two dimensional microcoil, the chemical was released at the targeted spatial location since the gel encapsulated within it was softened. The localized remote-controlled chemical delivery establishes a methodology for remotely manipulating the chemical and biological micro-environment for applications in cell engineering, tissue engineering, and drug development. A similar technology was applied to demonstrate a low temperature method for enabling truly three dimensional encapsulations of cells, embryos, and eggs with porosity that can be precisely engineered on all faces in three dimensions that facilitates better transport of media and nutrients [37].

4. Self-Assembly of Nanoscopic Objects

In this section, we present a list of selected examples on the use of micro- and nanofluidic assisted self-assembly for a range of nanoscopic organic and inorganic materials. The size and types of materials, the principles and methodologies as well as their novel applications will be emphasized for each example.

4.1. Organic

4.1.1. Monodisperse Lipid-Polymer and Lipid-Quantum Dot Nanoparticles

Continuous flow-based microfluidic synthesis is also useful for the synthesis of multicomponent nano-particles for therapy or diagnosis by obtaining reproducible monodisperse nanoparticles with a minimum number of preparation steps. The conventional methods for synthesizing lipid-polymeric nanoparticles are complex and require steps such as heating, vortexing, and long incubation times, which do not make the process easily amenable to combinatorial synthesis and can introduce variability in the properties of nanoparticles. Recently, Valencia *et al.* reported the use of microfluidic rapid mixing using hydrodynamic flow focusing in combination with passive mixing structures to realize the self-assembly of monodisperse lipid-polymer and lipid-quantum dot nanoparticles in a single mixing step [41]. These nanoparticles were composed of a polymeric core for drug encapsulation or a quantum dot core for imaging purpose, a hydrophilic shell, and a lipid monolayer at the interface between the core and the shell. At the junction of the streams, the polymeric or quantum dot solution was hydrodynamically focused by two lipid solutions and enhanced mixing occurred through the Tesla structures as the focused streams flow along the channel. In contrast to the slow mixing of lipid and polymeric solutions, rapid mixing promotes the formation of homogeneous nanoparticles with relatively narrow distribution, thereby eliminating the need for subsequent thermal or mechanical agitation for homogenization. This technology could greatly facilitate combinatorial synthesis and prove to be useful in the emerging field of nano-medicine.

4.1.2. Tubular and Hollow Organic Conductive Nanowires

Continuous flow-based microfluidic synthesis continues to be an important tool for nanomaterial synthesis, in this case, the formation of organic conductive nanowires in a fast one-step process. Puigmartí-Luis *et al.* developed a new method based on microfluidic-dictated self-assembly to promote the formation of a structurally defined and electrically conductive hybrid material in a fast and facile method [79]. The microreactor used is shown in Figure 9. Tetrathiafulvalene (TTF) based solution, a widely used monomer for synthesizing numerous organic conductors and complex small self-assembled structures with intriguing electrical and optical properties, together with other associated reactant and sheath solutions were loaded in each inlet in a PDMS based planar microfluidic device to experience co-flowing. Due to the laminar flow, the compound mixed by diffusion only and the reactions took place with preference either directly at, or with close proximity to the interface of the two inner streams. By changing the length of the microchannels, the flow rates, and the ratio of the reactants, different diameters (200 to 400 nm) and lengths (10 to 40 μm) of the tubular and hollow nanowires were obtained with different crystalline structures. With the presence of gold, the wires could act as a mediated template support for adhering molecules or other nanocomposites to allow for new applications such as hybrid sensor system.

Figure 9. (**a**) Microscopy image of the microreactor used for the synthesis. Each input channel is indicated with arrows. A and D are the sheath flows, B and C the reactant flows. (**b**,**c**) Finite element analysis simulation illustrating the microfluidic chip design and the concentration profiles of the reactants along the microchannel at a flow-rate ratio of (**b**) 0.1 and (**c**) 10 and a total flow rate of 1100 μL/min (top view, red stream: TTF, light-blue stream: Au, dark-blue streams: acetonitrile sheath flows). (**d**) Scheme illustrating the supramolecular organization of the composites (Reproduced with permission from [79]. Copyright 2010 Wiley-VCH Verlag GmbH & Co. KGaA).

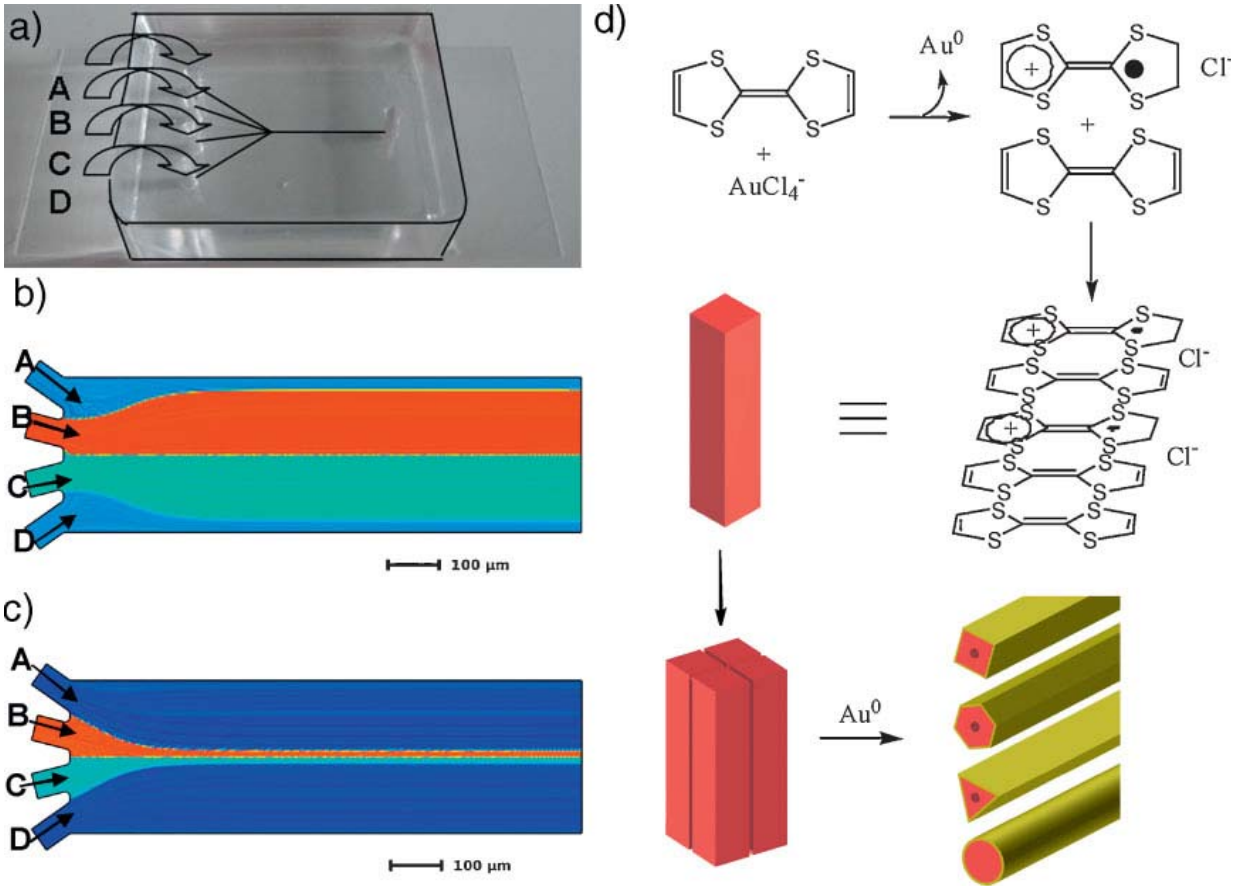

4.1.3. Lipid Membranes

Membrane channel proteins are of great interest as subjects of basic biophysical study, targets of high-throughput assays for drug discovery [80] and atomically precise nanopores for molecular sensing [81], and oligonucleotide analysis [82]. However, their widespread application to these areas has been limited by difficulties in fabricating planar lipid bilayer membranes. Previous approaches to microfluidic lipid membrane formation were based on the microfabricated orifices in microfluidic channels made from poly(methyl methacrylate) [83], but suffered from a number of disadvantages. Attention from an operator is necessary to manipulate the device during membrane formation, which is operator-intensive and not amenable to automation. Malmstadt *et al*. proposed a new microfluidic approach for forming these sub-5 nm-thick free-standing structures based on a self-assembly process driven by solvent extraction in a microfluidic channel [84]. This facile automatable process forms

high-quality membranes able to host channel proteins measurable at single-molecule conductance resolution. Figure 10 shows the principle of operation of lipid-bilayer formation by solvent extraction. It requires first the establishment of a biphasic flow in a PDMS channel. A droplet of nonpolar solvent containing dissolved lipid is formed in an aqueous flow stream. The amphiphilic lipids assemble on the aqueous-organic interface. Because the organic solvent is in contact with the PDMS from which the channel is fabricated, the solvent will partition into the bulk of the device. Lipids, however, do not partition into PDMS. As solvent is extracted from the lipid solution droplet, the droplet becomes smaller, bringing the two lipid-coated aqueous-organic interfaces closer together. Finally, the solvent is completely extracted, bringing the lipid layers together, forming a bilayer membrane.

Figure 10. Mechanism for lipid bilayer formation by microfluidic solvent extraction. (**a**) A droplet of organic solvent with dissolved lipid is formed in an aqueous stream of fluid. Lipids are organized on the hydrophobic-hydrophilic interface (inset). (**b**) As solvent enters the PDMS, the two interfaces approach one another. (**c**) Finally, only the lipid layers are left behind, forming a bilayer membrane. (Reprinted with permission from [84]. Copyright 2006 American Chemical Society).

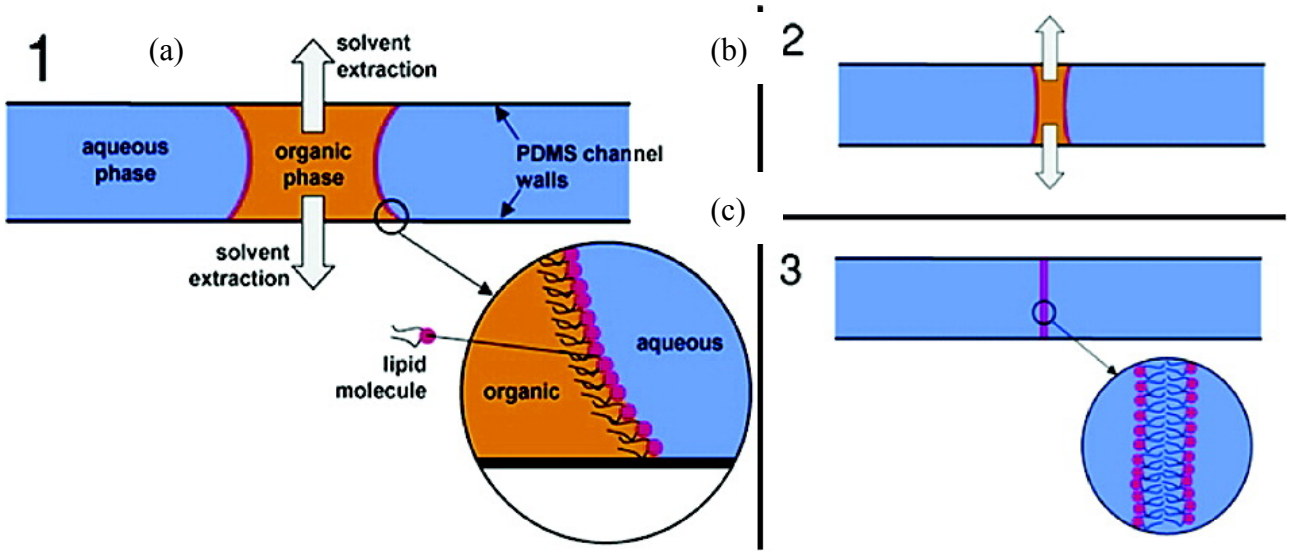

Recently, a bilayer formation method based on mechanical union of self-assembled lipid monolayers has simplified the process of bilayer formation within microfluidic devices leading to the possibility of extremely high throughput [85]. Also, Aghdaei *et al.* recently used dielectrophoresis to drive bilayer formation in a microfluidic device [43]. Poulos *et al*. proposed a similar method, developing a new microfluidic device that combines the electrowetting on dielectric driving mechanism with on-chip thin-film electrodes for parallel formation and measurement of artificial lipid bilayer arrays [86]. Electrowetting is used to facilitate the contact of separate aqueous droplets immersed within a lipid containing alkane solution, resulting in functional lipid bilayer membranes able to host ion channels. The contacting monolayer method on an electrowetting on dielectric chip with integrated Ag/AgCl electrodes represents an attractive and scalable platform that allows automated formation of lipid bilayers and simultaneous monitoring of ion channels in an array format.

4.1.4. DNA-origami

DNA-origami technology [30] is a well-developed method to create fully addressable DNA nanostructures by using approximately 200 short staple DNA strands to fold a single-strand of genomic DNA into geometrically defined nanopatterns. Based on this technique, the DNA-guided self-assembly of noble-metal nanoparticles (NPs) with nanometer-scale precision has shown significant progress [87], which is an important goal in nanotechnology. Enormous progress has been made in the DNA-guided organization of nanoparticles into discrete [88], one-dimensional [89], two-dimensional [90], and three-dimensional architectures [91]. Facile DNA-functionalization strategies for gold nanoparticles (AuNPs) are now available, making AuNPs preferred candidates for subsequent self-assembly to form higher-order structures.

Instead of AuNPs, Pal *et al.* proposed a new bottom-up method for the fabrication of discrete, well-ordered AgNP nanoarchitectures on self-assembled DNA origami structures of triangular shape by using AgNPs (20 nm in diameter) conjugated with chimeric phosphorothioated DNA (ps-po DNA) as building blocks [92]. They exploited the organizational power of DNA origami to develop a robust strategy for the assembly of otherwise hard-to-control AgNPs into well-defined nanoarchitectures. As AgNPs possess unique optical properties (for example, the local surface plasmon resonance (LSPR) effect is stronger between AgNPs than between AuNPs), the strategies demonstrated herein could potentially lead to useful photonic structures enabled by the spatial control of AgNP structures. Maune *et al.* also proposed a new bottom-up general method for arranging single-walled carbon nanotubes in two dimensions using DNA origami [93]. They synthesized rectangular origami templates (~75 nm × 395 nm) that displayed two lines of single-stranded DNA 'hooks' in a cross pattern with ~6 nm resolution. The perpendicular lines of hooks served as sequence-specific binding sites for two types of nanotubes, each functionalized noncovalently with a distinct DNA linker molecule. The hook-binding domain of each linker was protected to ensure efficient hybridization. When origami templates and DNA-functionalized nanotubes were mixed, strand displacement-mediated deprotection and binding aligned the nanotubes into cross-junctions. Thus, DNA origami may allow the rapid prototyping of complex nanotube-based structures.

4.1.5. Lipid Vesicles

The drive for miniaturization to reduce sample consumption and increase throughput has mainly been addressed by microfabrication but this method cannot fulfill the demand for studying the chemical reactions inside biological cells that occurs on three dimensional length scales ranging from several micrometers to nanometers, as dictated by the dimensions of cells and their intracellular compartments. Bolinger *et al.* recently employed self-assembly to create a nanofluidic system for mixing attoliter volumes (released from nanometer-sized lipid vesicles) in a closed femtoliter reactor vessel (a larger unilamellar lipid vesicles), thereby controlling the number of mixed reactants with single-molecule precision [94]. The mixing of reactants, which initiates an enzyme-catalyzed transformation of nonfluorescent substrate to a fluorescent product, was triggered by changes of temperature that drive the small vesicles through phase transition. To monitor the function of the individual reactor systems in a parallel manner, these biotinylated nanoreactors were immobilized on a

solid support functionalized with neutravidin. The technology offers the possibility for advanced synthetic biology study and the realization of artificial cells.

4.1.6. Carbon Nanotubes

Shim *et al.* recently reported the fluidic self-assembly of carbon nanotubes (CNT) using magnetically capturing residual iron (Fe) catalyst as shown in Figure 11 [95]. The Fe catalyst provides a seeding site on one end of the CNT after the synthesis. Using a Ni pattern on the electrode, this Fe catalyst is magnetically attracted to the edge of Ni pattern. The assembled CNT is finally aligned parallel to the flow direction by fluidic shear force. As a result, this technique can be applied to fabricate a highly sensitive biosensor using specifically functionalized CNT. Xiong *et al.* accomplished this by capillary force that can be used to produce surface-controlled microfluidic approach for the fabrication of highly organized single walled carbon nanotubes (SWCNT) networks in various dimensions and geometries using the template assisted self-assembly method as schematically shown in Figure 12 [36,96].

Some carbon nanotubes were pulled out of solution into a pipette and deposited on a spinning silica substrate where they naturally stick, partly because of static electricity. By combining the gradient concentric ring and controlled ‘‘stick-slip’’ motion, evaporation-induced self-assembly of polymers in a sphere-on-flat geometry coupled with subsequent directed self-assembly of multi walled carbon nantubes on the polymer-templated surfaces was observed [97]. In addition to that, Valentini *et al.* introduced a simple technique whereby controlling the wettability of a conducting surface and the dip-coating speed, it is possible to build highly organized SWCNT based architectures [98].

Figure 11. The carbon nanotube (CNT) is aligned parallel to the flow direction (Reprinted with permission from [95]. Copyright 2009 Institute of Physics).

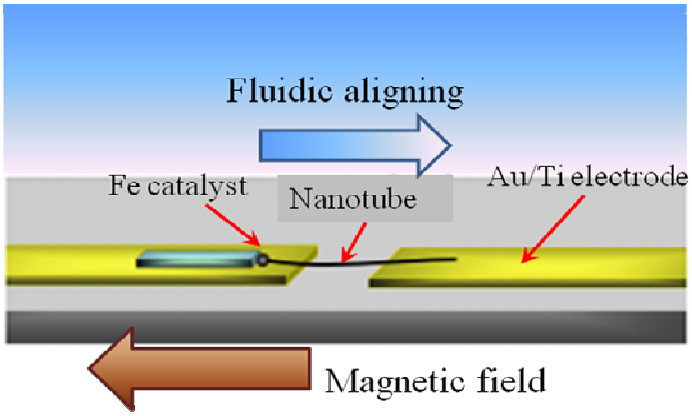

Figure 12. Schematic illustration of single walled carbon nanotubes (SWCNT) aggregation and assembly in channels by capillary induced flow, where the left vertical arrow denotes the template pulling direction and the two right ones represent the sweeping direction of the liquid–solid contact line in poly(methyl methacrylate) (PMMA) channels (Reproduced with permission from [36]. Copyright 2007 Wiley-VCH Verlag GmbH & Co. KGaA.).

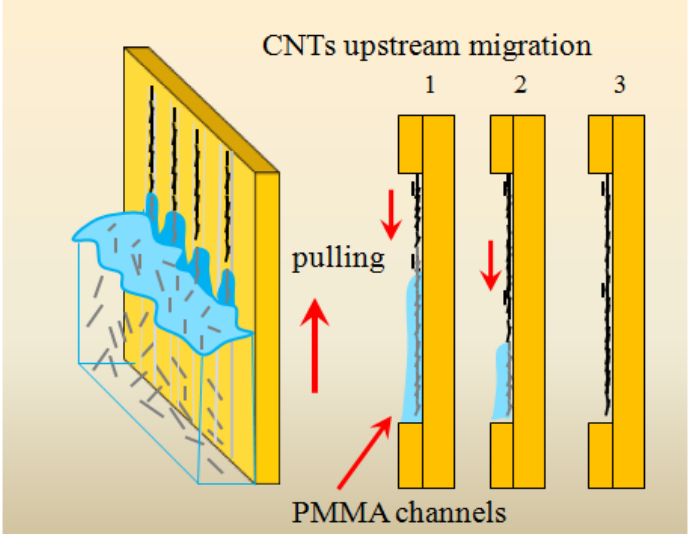

4.1.7. Organic Nanoparticles

As mentioned above, continuous flow-based microfluidics is an important tool for nanomaterial synthesis. However, at this small scale, surface forces and surface properties such as surface tension, the physical or chemical interaction between reactants and surface and the roughness of the surface become more significant than the particle motion. This can cause the deposition of nanoparticles or even clogging problems in the microchannel that can hinder the production of nanoparticles of controlled size. One way to solve the problem is the use of 3D fluidic geometries, as well as coaxial flow and 3D hydrodynamic focusing. Génot *et al.* recently employed this method to synthesize rubrene nanocrystals through a non-solvent crystallization process [99]. A glass capillary tube was inserted into the microreactor where rubrene with its solvent was flowed through it and the side flows (organic solution with water) were applied to surround the centrally located rubrene flow which formed a 3D coaxial flow. The design successfully controlled the supersaturation level while manipulated mixing conditions, and avoided fouling and clogging within the main channel. By varying the focusing ratio between side and capillary inlet flows, the mean size of the nanocrystals can be controlled. This 3D coaxial flow concept has also been applied to synthesize other types of micro- and nanomaterials such as polymeric microparticles [100] and thiol functionalized gold nanoparticles [101].

4.2. Inorganic

4.2.1. Silica Nano-Particles

Although high quality colloidal films with minimal lattice defects and large domain size have been achieved as mentioned above, success in many applications also demand the ability to pattern self-assembled colloidal lattices in well-defined architectures and within integrated micro-systems.

Recently, Zeng *et al.* employed multiple evaporation micro-channels to reduce the stress nonuniformity by dividing wide open edges into segments shorter than the characteristic length scale above which cracking occurs and prevent the drying front from penetrating into the bulk [13]. They successfully self-assembled 330 nm silica nanoarrays with no cracks in a 4 mm^2 square chamber connected to the reservoirs via 20 microchannels on each side. The micro-system was then tested for high-throughput separation of 2–50 kbp DNA based on continuous-flow separation under asymmetric pulsed electric fields.

Based on a similar method, Zeng *et al.* developed a gel-free biomolecular sieving system based on the use of three dimensional ordered colloidal arrays to define the sieve structure within a microfluidic device [102]. The process of microfluidic colloidal self-assembly was conducted by opening only a reservoir connected to a microchannel so that evaporation induced colloidal growth occurred within the micro-channel. Different pore sizes of about 135, 50, and 24 nm were constructed based on particle diameters of 900, 330, and 160 nm, respectively. The ability of accessing a wide range of pore sizes allowed them to adjust the separation performance for a given type of biomolecule, ranging from proteins smaller than 10 nm to micrometer-sized long DNA coils.

Self-assembly of colloidal nanospheres can also be applied for the production of nanofluidic filter. Seo demonstrated a facile method to fabricate the nanomesh fluidic filter in the local region of the microchannel by self-assembly of colloidal nanospheres and surface tension [103]. A droplet of colloid on the entrance of the microchannels forms the colloid plug because of the surface tension. The silica nanospheres with diameter of about 567 nm were orderly packed by the capillary force driven by the evaporating liquid flow after the liquid in the colloid was evaporated and the porosity and nanopore diameter were about 45.4% and 158 nm, respectively. The advantages of this method include no nanoscale photomask being required, the pore size of the nanofluidic filter can be controlled by changing the nanosphere size, and it can be easily integrated in the microchannel.

Nanochannels with feature sizes comparable to Debye length exhibit fascinating ionic transport characteristics due to the overlapped electrical double layers and have attracted a lot of research in nanofluidics in recent years [104-106]. Based on this phenomenon, Lei *et al.* recently developed an interesting nanofluidic diode in a suspended silica nanoparticle crystal (S-NPC) constructed by sequentially packing hydroxyl-modified and amino-modified nanoparticles into a microfabricated silicon micropore as shown in Figure 13 [107]. Both types of nanoparticles with diameter as small as 173 nm were loaded from opposite sides into the micropore and with the help of evaporation induced self-assembly, nanoparticle crystal was formed. Current rectification in these nanofluidic diodes comes from the asymmetric surface charge polarities along the nanochannel network inside the nano-particle crystal. This type of nanofluidic diode will find applications in biosensing due to its excellent electrical performance, the ease of surface charge formation, and low cost.

Figure 13. Nanofluidic diode in a suspended silica nanoparticle crystal (S-NPC). Schematic illustrations of the present S-NPC nanofluidic diode (**a**) and its working principle (**b**). SEM images of a silicon micropore after assembly of the hydroxyl modified nanoparticles at one end (**c**), and a magnified view of the nanoparticles at the interface before the second set of nanoparticles were packed (**d**). (Reprinted with permission from [107]. Copyright 2010, American Institute of Physics).

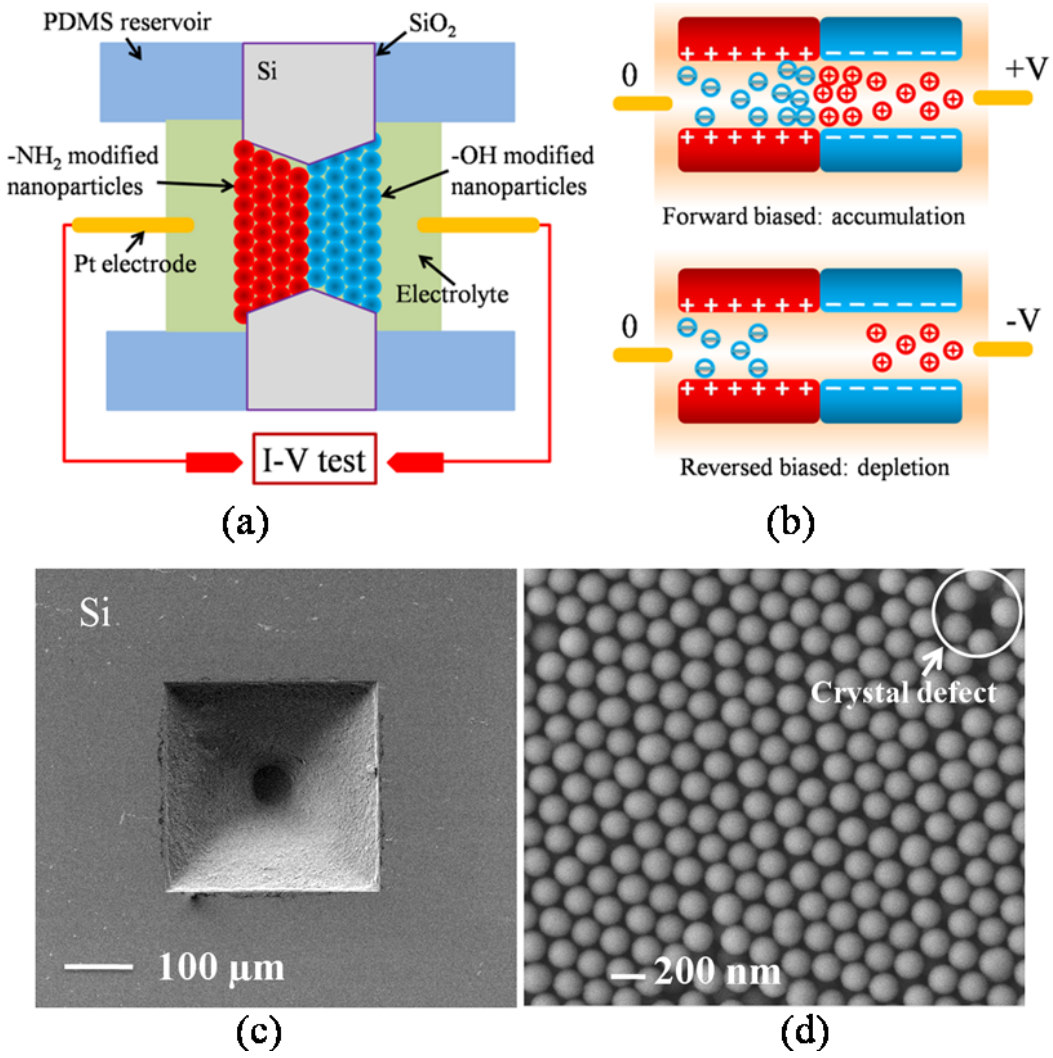

4.2.2. Hierarchical Isotropic and Anisotropic Metallic Nano-Structures

This capillary interaction at the solution surface can be extended into the self-assembly of nanometer and even subnanometer sized particles. It has been speculated that capillary interaction strength decreases with diminishing object dimension and the randomizing effects of the thermal fluctuation energy (*kT*) become more significant. Theoretically, the capillary interaction energy between two 2-nm-diameter particles with immersion configuration in water is less than *kT* [108]. A significant advancement of nanoscale self-assembly was demonstrated by Cui *et al.* [25]. They successfully assembled hierarchical isotropic and anisotropic colloidal nanostructures over large areas based on interfacial capillary force present during the evaporation of a nanocrystal suspension at the lithographically defined nanoconfinement. Reproducible organizations of 50-, 8- and 2-nm diameter of

gold and silver nanoparticles at precise location on the chip and/or within a circuit were achieved. In addition to that, complex nanostructures such as nanotetrapods and reproducible high-yield and high-selectivity fabrication of arrays of single-particle transistors by assembling nanoparticles into electrode gaps were demonstrated. The method is generic since capillary force is material-independent. Controlling the particle-water contact angle is crucial to the success of this assembly method because it determines the direction of the capillary force. The method is applicable to create highly integrated functional nanosystems such as tunable plasmon waveguides made of metal nanocrystal chains for nanophotonics.

4.2.3. Semiconductor Nanorods

Recently, the research on self-assembly of colloidal nanostructures has advanced tremendously by self-assembling colloidal semiconductor nanorods resulting in their device-scale perpendicular alignment. Baker *et al*. demonstrated a controlled-drying method to produce both short- and long-range order of cadmium sulfide (CdS) nanorod films which oriented vertically [109]. An unprecedented control over orientational order of up to 96% vertically oriented rods on 1 cm^2 area on a wide range of substrates was achieved. The kinetics on orientational order was found to play an important role in rod self-assembly. This advancement may play a critical role in the development of inexpensive, solution-processed optoelectronics with performance matching that of bulk semiconductor devices.

4.2.4. Metallic and Semiconductor Nanofibers and Nanowires

As mentioned above, researchers have utilized capillary, shear, electrostatic, dielectrophoretic, magnetic, and molecular forces to organize the assembly of synthesized colloids and nanostructures onto surfaces [110] where they can serve as the active element or as a mask for deposition of other materials. The assembly of single silicon nanowires with high yield (98.5%) over a large number of electrode sites (>16,000) was demonstrated as schematically shown in Figure 14 [111]. Alignment of nanochannels with similar precision could be achieved in the near future since nanochannels are formed by simply etching nanowires in their process. One example is the fabrication of nanoscale resonators from the dielectrophoretic assembly of semiconductor nanowires. Shear forces were also used to direct the assembly of nanowires incorporated into the architecture of flexible devices [112]. In addition to that, Fan *et al.* developed a combination of alternating and constant electric fields applied by means of lithographically patterned electrodes where gold nanowires were moved along any arbitrary trajectory with speeds up to 50 μm/s and positioned at an arbitrary location with a precision better than 300 nm [113]. Hybrid nanoelectromechanical systems array integration strategy which combined deterministic bottom-up silicon and rhodium nanowire assembly with conventional top-down microfabrication could also produce higher assembly yields (>80%) [114].

Figure 14. Nanowire self-assembly onto electrode arrays from solution. The foreground depicts a side view of fluid flow alignment of a colloidal suspension of nanowires that are subsequently trapped by dielectrophoretic forces between two opposite electrodes. The background illustrates a top view of the final array of assembled nanowires between electrode pairs (Reprinted by permission from [111]. Copyright 2010 Macmillan Publishers Ltd).

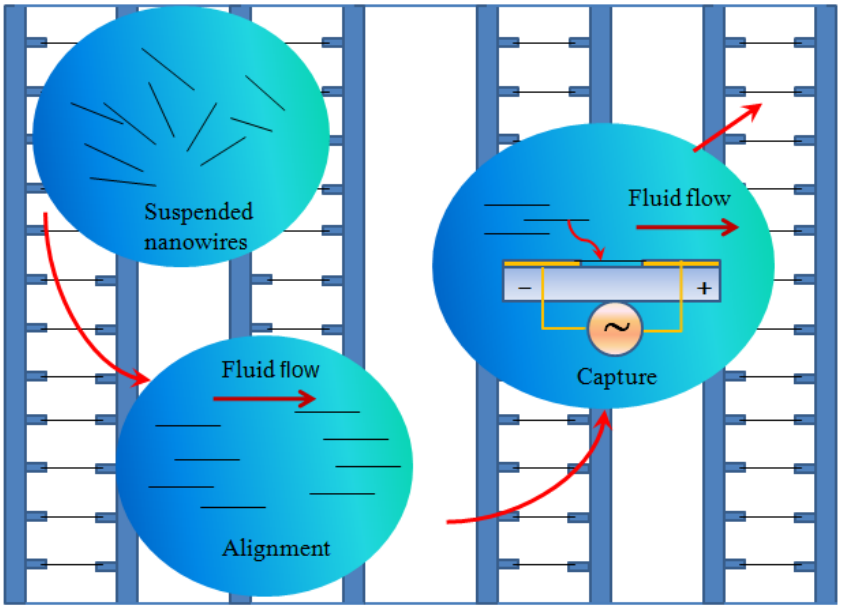

5. Conclusions and Perspectives

In summary, we describe the recent activities involving micro- and nanofluidic systems which prove to be useful platforms to assist the self-assembly of a variety of organic and inorganic micro- and nanomaterials with high throughput and controllable size, shape, pattern alignment, and size distribution. The examples presented here concentrate on the size and types of materials being assembled, the principles and methodologies as well as their novel applications. A wide range of micro- and nanoscopic objects with different shapes (spherical, nonspherical, complex, thin film, rectangular, 3D container, tubular, hollow, and 1D nanorod) and material properties (polymers, biological entities, silica, para and superparamagnetic, conductive organic, semiconductor, metallic, carbon) have been successfully self-assembled in two- and three-dimensions. Free-flow self-assembly, hydrodynamic coflowing self-assembly such as droplet flow, plug flow, and laminar flow, and other emerging new microfluidic technologies such as railed microfluidic self-assembly and droplet based electrowetting are promising ways for large scale, parallel fabrication of devices made up of many small components. These micro- and nanofluidic assisted self-assembly methods have provided a wide range of novel applications in the areas of micro- and nanoelectronic, biomedical, optics, sensors, cell study, and actuators. Some of the best examples include the self-assembly of amphiphilic, nonspherical, polymeric microparticles with the ability to assemble into a wide range of crystal structures unavailable to spheres, and their anisotropy-driven response to interfacial forces and external fields creates many new applications in drug delivery and pharmaceutical applications. Another example is the fabrication of three dimensional microstructures by using the power of cells, a truly interesting

example that employs biological entities to do the job. The third example involves the well-controlled self-assembly of isotropic and anisotropic metallic nanostructures and carbon nanotubes into electronic networks that surely will provide unprecedented performance of highly efficient and sensitive biosensing and nanoelectronics. These three excellent examples show typical highly-sought after breakthroughs in some of the current and most important research areas in polymer, biological, and electronics. Hence, the continuous development in microfluidic assisted self-assembly is foreseen.

Although only a few nanofluidic related self-assembly methods have been demonstrated, possibly due to nanofabrication complexity and fundamental issues encountered, it will be excited to see new advancements and breakthroughs in the near future. Nanofluidic assisted self-assembly is unique since powerful nanofluidic devices can be envisioned if all the essential nanoanalytical components such as nanoelectronics, nanooptics, and nanoelectrochemistry can be "nanofluidically" self-assembled and integrated. We can then analyze, separate, concentrate, manipulate and detect biomolecules with better sensitivity and higher speed, allow unique DNA sequencing, and finally enable novel biomolecular detection methods due to some underlying basic nanoscale phenomena.

References and Notes

1. Brenner, S.L.; Zlotnick, A.; Griffith, J.D. RecA protein self-assembly. Multiple discrete aggregation states. *J. Mol. Biol.* **1988**, *204*, 959-972.
2. Braun, P.V. Natural nanobiocomposites, biomimetic nanocomposites, and biologically-inspired nanocomposites. In *Nanocomposite Science and Technology*; Ajayan, P.M., Schadler, L.S., Braun, P.V., Eds.; Wiley-VCH: Weinheim, Germany, 2003.
3. Park, J.; Joo, J.; Kwon, S.G.; Jang, Y.; Hyeon, T. Synthesis of monodisperse spherical nanocrystals. *Angew Chem. Int. Ed.* **2007**, *46*, 4630-4660.
4. Vayssieres, L. Growth of arrayed nanorods and nanowires of ZnO from aqueous solutions. *Adv. Mater.* **2003**, *15*, 464-466.
5. Wiley, B.J.; Chen, Y.; McLellan, J.M.; Xiong, Y.; Li, Z.-Y.; Ginger, D.; Xia, Y. Synthesis and optical properties of silver nanobar. *Nano Lett.* **2007**, *7*, 1032-1036.
6. Daniel, M. C.; Astruc, D. Gold nanoparticles: Assembly, supramolecular chemistry, quantum-size-related properties, and applications toward biology, catalysis, and nanotechnology. *Chem. Rev.* **2004**, *104*, 293-346.
7. Skrabalak, S.E.; Chen, J.; Sun, Y.; Lu, X.; Au, L.; Cobley, C. M.; Xia, Y. Gold nanocages, synthesis, properties, and applications. *Acc. Chem. Res.* **2008**, *41*, 1587-1595.
8. Trindade, T.; O'Brien, P.; Pickett, N.L. Nanocrystalline semiconductors: synthesis, properties, and perspective. *Chem. Mater.* **2001**, *13*, 3843-3858.
9. Sun, S.H.; Zeng, H. Size-controlled synthesis of magnetic nanoparticles. *J. Am. Chem. Soc.* **2002**, *124*, 8204-8205.
10. Khoo, H.S.; Tseng, F.-G. Engineering the 3D architecture and hydrophobicity of methyltrichlorosilane nanostructures. *Nanotechnology* **2008**, *19*, 345603.
11. Wang, J.; Patel, M.; Gracias, D.H. Self-assembly of three-dimensional nanoporous containers. *Nano* **2009**, *4*, 1-5.

12. Nie, Z.; Li, W.; Seo, M.; Xu, S.; Kumacheva, E. Janus and ternary particles generated by microfluidic synthesis: design, synthesis, and self-assembly. *J. Am. Chem. Soc.* **2006**, *128*, 9408-9412.
13. Zeng, Y.; He, M.; Harrison, D.J. Microfluidic self-patterning of large-scale crystalline nanoarray for high-throughput continuous DNA fractionation. *Angew. Chem. Int. Ed.* **2008**, *47*, 6388-6391.
14. Hong, J.S.; Stavis, S.M.; DePaoli Lacerda, S.H.; Locascio, L.E.; Raghavan, S.R.; Gaitan, M. Microfluidic directed self-assembly of liposome-hydrogel hybrid nanoparticles. *Langmuir* **2010**, *26*, 11581-11588.
15. Qin, D.; Xia, Y.; Whitesides, G.M. Rapid prototyping of complex structures with feature sizes larger than 20 μm. *Adv. Mater.* **1996**, *8*, 917-919.
16. Xia, Y.; Whitesides, G.M. Soft lithography. *Angew. Chem. Int. Ed.* **1998**, *37*, 550-575.
17. Duraiswamy, S.; Khan, S.A. Plasmonic nanoshell synthesis in microfluidic composite foams. *Nano Lett.* **2010**, *10*, 3757-3763.
18. Mastrangeli, M.; Abbasi, S.; Varel, C.; Van Hoof, C.; Celis, J.-P.; Böhringer, K.F. Self-assembly from milli- to nanoscale: methods and applications. *J. Micromech. Microeng.* **2009**, *19*, 083001.
19. Mann, S. Self-assembly and transformation of hybrid nano-objects and nanostructures under equilibrium and non-equilibrium conditions. *Nat. Mater.* **2009**, *8*, 781-792.
20. Ariga, K.; Hill, J.P.; Lee, M.V.; Vinu, A.; Charvet, R.; Acharya, S. Challenges and breakthroughs in recent research on self-assembly. *Sci. Technol. Adv. Mater.* **2008**, *9*, 014109.
21. Bishop, K.J. M.;Wilmer, C.E.; Soh, S.; Grzybowski, B.A. Nanoscale forces and their uses in self-assembly. *Small* **2009**, *5*, 1600-1630.
22. Squires, T.M.; Quake, S.R. Microfluidics: Fluid physics at the nanoliter scale. *Rev. Mod. Phys.* **2005**, *77*, 977-1026.
23. Sparreboom, W.; van den Berg, A.; Eijkel, J.C.T. Transport in nanofluidic systems: A review of theory and applications. *New J. Phys.* **2010**, *12*, 015004.
24. Huang, S.H.; Khoo, H.S.; ChangChien, S.Y.; Tseng, F.G. Synthesis of bio-functionalized copolymer particles bearing carboxyl groups via a microfluidic device. *Microfluid. Nanofluid.* **2008**, *5*, 459-468.
25. Cui, Y.; Björk, M.T.; Liddle, J.A.; Sönnichsen, C.; Boussert, B.; Alivisatos, A.P. Integration of colloidal nanocrystals into lithographically patterned devices. *Nano Lett.* **2004**, *4*, 1093-1098.
26. Sivagnanam, V.; Song, B.; Vandevyver, C.; Bünzli, J.-C.G.; Gijs, M.A.M. Selective breast cancer cell capture, culture, and immunocytochemical analysis using self-assembled magnetic bead patterns in a microfluidic chip. *Langmuir* **2010**, *26*, 6091-6096.
27. Wu, L.Y.; Carlo, D.D.; Lee, L.P. Microfluidic self-assembly of tumor spheroids for anticancer drug discovery. *Biomed. Microdevices* **2008**, *10*, 197-202.
28. Ormonde, A.D., Hicks, E.C.M., Castillo, J.; Duyne, R.P.V. Nanosphere lithography: Fabrication of large-area Ag nanoparticle arrays by convective self-assembly and their characterization by scanning UV—visible extinction spectroscopy. *Langmuir* **2004**, *20*, 6927–6931.
29. Salalha, W.; Zussman, E. Investigation of fluidic assembly of nanowires using a droplet inside microchannels. *Phys. Fluids* **2005**, *17*, 063301.
30. Rothemund, P.W.K. Folding DNA to create nanoscale shapes and patterns. *Nature* **2006**, *440*, 297-302.

31. Leong, T.G.; Benson, B.R.; Call, E.K.; Gracias, D.H. Thin film stress driven self-folding of microstructured containers. *Small* **2008**, *10*, 1605-1609.
32. Onoe, H.; Takeuchi, S. Microfabricated mobile microplates for handling single adherent cells. *J. Micromech. Microeng.* **2008**, *18*, 095003-095010.
33. Choi, S.; Park, I.; Hao, Z.; Holman, H.-Y.N.; Pisano, A.P.; Zohdi, T.I. Ultrafast self-assembly of microscale particles by open-channel flow. *Langmuir* **2010**, 26, 4661-4667.
34. Bleil, S.; Marr, D.W.M.; Berchinger, C. Field-mediated self-assembly and actuation of highly parallel microfluidic devices. *Appl. Phys. Lett.* **2006**, *88*, 263515.
35. Xiong, X.; Hanein, Y.; Fang, J.; Wang, Y.; Wang, W.; Schwartz, D. T.; Böhringer, K. F. Controlled multibatch self-assembly of microdevices . *J. Microelectromech. Syst.* **2003**, *12*, 117-27.
36. Xiong, X.; Laila Jaberansari, L.; Hahm, M.G.; Busnaina, A.; Jung, Y.J. Building highly organized single-walled-carbon-nanotube networks using template-guided fluidic assembly. *Small* **2007**, *3*, 2006 -2010.
37. Leong, T.G.; Randall, C.L.; Benson, B.R.; Zarafshar, A.M.; Gracias, D.H. Self-loading lithographically structured microcontainers: 3D patterned, mobile microwells. *Lab Chip* **2008**, *8*, 1621-1624.
38. Zheng, B.; Tice, J.D.; Ismagilov, R.F. Formation of droplets of alternating composition in microfluidic channels and applications to indexing of concentrations in droplet-based assays. *Anal. Chem.* **2004**, *76*, 4977-4982.
39. Ota, S.; Yoshizawa, S.; Takeuchi, S. Microfluidic Formation of monodisperse, cell-sized, and unilamellar vesicles. *Angew. Chem. Int. Ed.* **2009**, *48*, 6533-6537.
40. Chung, K.-Y.; Mishra, N.C.; Wang, C.-C.; Lin, F.-H.; Lin, K.-H. Fabricating scaffolds by microfluidics. *Biomicrofluidics* **2009**, *3*, 022403.
41. Valencia, P.M.; Basto, P.A.; Zhang, L.; Rhee, M., Langer, R.; Farokhzad, O.C.; Karnik, R.S. Single-step assembly of homogeneous lipid-polymeric and lipid-quantum dot nanoparticles enabled by microfluidic rapid mixing. *ACS Nano* **2010**, *4*, 1671-1679.
42. Chung, S.E.; Park, W.; Shin, S.; Lee, S.A.; Kwon, S. Guided and fluidic self-assemlby of microstructures using railed microfluidic channels. *Nat. Mater.* **2008**, *7*, 581-587.
43. Aghdaei, A.; Sandison, M. E.; Zagnoni, M.; Green, N.G.; Morgan, H. Formation of artificial lipid bilayers using droplet dielectrophoresis. *Lab Chip* **2008**, *8*, 1617-1620.
44. Perro, A.; Reculusa, S.; Ravaine, S.; Bourgeat-Lami, E.; Duguet, E. Design and synthesis of Janus micro- and nanoparticles. *J. Mater. Chem.* **2005**, *15*, 3745-3760.
45. Vanakaras, A.G. Self-organization and pattern formation of janus particles in two dimensions by computer simulations. *Langmuir* **2006**, *22*, 88-93.
46. Yuet, K.P.; Hwang, D.K.; Haghgooie, R.; Doyle, P.S. Multifunctional superparamagnetic janus particles. *Langmuir* **2010**, *26*, 4281-4287.
47. Lu, Y.; Yin, Y.; Xia, Y. Three-dimensional photonic crystals with non-spherical colloids as building blocks. *Adv. Mat.* **2001**, *13*, 415-420.
48. Dendukuri, D.; Hatton, T. A.; Doyle, P.S. Synthesis and self-assembly of amphiphilic polymeric microparticles. *Langmuir* **2007**, *23*, 4669-4674.

49. Stroock, A.D.; Dertinger, S.K.; Whitesides, G.M.; Ajdari, A. Patterning flows using grooved surfaces. *Anal. Chem.* **2002**, *74*, 5306-5312.
50. Chung, S.E.; Park, W.; Park, H.; Yu, K.; Park, N.; Kwon, S. Optofluidic maskless lithography system for real-time synthesis of photopolymerized microstructures in microfluidic channels. *Appl. Phys. Lett.* **2007**, *91*, 041-106.
51. Lee, A.S.; Chung, S.E.; Park, W.; Lee, S.H.; Kwon, S. Three-dimensional fabrication of heterogeneous microstructures using soft membrane deformation and optofluidic maskless lithography. *Lab Chip* **2009**, *9*, 1670-1675.
52. Chung, S.E.; Lee, S.A.; Kim, J.; Kwon, S. Optofluidic encapsulation and manipulation of silicon microchips using image processing based optofluidic maskless lithography and railed microfluidics. *Lab Chip* **2009**, *9*, 2845-2850.
53. Park, W.; Lee, H.; Park, H; Kwon, S. Sorting directionally oriented microstructures using railed microfluidics. *Lab Chip* **2009**, *9*, 2169-2175.
54. Kuribayashi, K.; Onoe, H.; Takeuchi, S. Assembly of 3d microstructures powered by cells. *Thirteenth International Conference on Miniaturized Systems for Chemistry and Life Sciences*, Jeju, Korea, November 2009; pp. 1321-1323.
55. Lasic, D.D.; Papahadjopoulos, D. Liposomes revisited. *Science* **1995**, *267*, 1275-1276.
56. Tamba, Y.; Yamazaki, M. Single giant unilamellar vesicle method reveals effect of antimicrobial peptide Magainin 2 on membrane permeability. *Biochemistry* **2005**, *44*, 15823-15833.
57. Noireaux, V.; Libchaber, A. A vesicle bioreactor as a step toward an artificial cell assembly. *Proc. Natl. Acad. Sci. USA* **2004**, *101*, 17669-17674.
58. Funakoshi, k.; Suzuki, H.; Takeuchi, S. Formation of giant lipid vesiclelike compartments from a planar lipid membrane by a pulsed jet flow. *J. Am. Chem. Soc.* **2007**, *129*, 12608-12609.
59. Shum, H.C.; Lee, D.; Yoon, I.; Kodger, T.; Weitz, D.A. Double emulsion template monodisperse phospholipid vesicles. *Langmuir* **2008**, *24*, 7651-7653.
60. Desoize, B. Contribution of three-dimensional culture to cancer research. *Crit. Rev. Oncol. Hematol.* **2000**, *36*, 59-60.
61. Negishi, M.K.; Tsuda, Y.; Onoe, H.; Takeuchi, S. A neurospheroid network-stamping method for neural transplantation to the brain. *Biomaterials* **2010**, *31*, 8939-8945.
62. Yin, Y.; Lu, Y.; Gates, B.; Xia, Y. Template-assisted self-assembly: A practical route to complex aggregates of monodispersed colloids with well-defined sizes, shapes, and structures. *J. Am. Chem. Soc.* **2001**, *123*, 8718-8729.
63. Su, G.; Guo, Q.; Palmer, R.E. Colloidal lines and strings. *Langmuir* **2003**, *19*, 9669-9671.
64. Golding, R.K.; Lewis, P.C.; Kumacheva, E. *In situ* study of colloid crystallization in constrained geometry. *Langmuir* **2004**, *20*, 1414-1419.
65. Vilfan, M.; Potočnik, A; Kavčič, B.; Osterman, N.; Poberaj, I.; Vilfan, A.; Babič, D. Self-assembled artificial cilia. *Proc. Natl. Acad. Sci. USA* **2010**, *107*, 1844-1847.
66. Morris, C.J.; Stauth, S.A.; Parviz, B.A. Self-assembly for microscale and nanoscale packaging: Steps toward self-packaging. *IEEE Trans. Adv. Packag.* **2005**, *28*, 600-611.
67. Cohn, M.B.; Böhringer, K.F.; Noworolski, J.M.; Singh, A.; Keller, C.G.; Goldberg, K.Y.; Howe, R.T. Microassembly technologies for MEMS. In *Proceedings of SPIE Micromachining and Microfabrication*, Santa Clara, CA, USA, 1998; pp. 2-16.

68. Srinivasan, U.; Liepmann, D.; Howe, R.T. Microstructure to substrate self-assembly using capillary forces. *J. Microelectromech. Syst.* **2001**, *10*, 17-24.
69. Reynolds, K.; O'Riordan, A.; Redmond, G. Self-assembly of a functional electronic circuit directed by capillary interactions. *Appl. Phys. A* **2010**, *98*, 203-209.
70. Liu, M.; Lu, Y.; Zhang, J.; Xia, S.; Yang, J. MEMS/microelectronics self-assembly based on analogy of Langmuir—Blodgett approach. *Microelectron. Eng.* **2009**, *86*, 2279-2282.
71. Knuesel, R.J.; Jacobs, H.O. Self-assembly of microscopic chiplets at a liquid–liquid–solid interface forming a flexible segmented monocrystalline solar cell. *Proc. Natl. Acad. Sci. USA* **2010**, *107*, 993-998.
72. Fukushima, T.; Iwata, E.; Konno, T.; Bea, J.C.; Lee, K.W.; Tanaka, T.; Koyanagi, M. Surface tension-driven chip self-assembly with load-free hydrogen fluoride-assisted direct bonding at room temperature for three-dimensional integrated circuits. *Appl. Phys. Lett.* **2010**, *96*, 154105.
73. Arase, H.; Nakagawa, T. Interfacial-energy-controlled deposition technique of microstructures using blade-coating. *J. Phys. Chem. B* **2009**, *113*, 15278–15283.
74. Lin, C.; Tseng, F.G.; Chieng, C.C. Studies on size and lubricant effects for fluidic self-assembly of microparts on patterned substrate using capillary effect. *J. Electron. Packag.* **2008**, *130*, 021005.
75. Lin, C.; Tseng, F. G.; Kan, H.C.; Chieng, C.C. Numerical studies on micropart self-alignment using surface tension forces. *Microfluid. Nanofluidics* **2009**, *6*, 63-75.
76. Lin, C.; Tseng, F.G.; Chieng, C.C. Orientation-specific fluidic self-assembly process based on a capillary effect. *J. Micromech. Microeng.* **2009**, *19*, 115020.
77. Cho, J.-H.; Gracias, D.H. Self-assembly of lithographically patterned nanoparticles. *Nano Lett.* **2009**, *9*, 4049-4052.
78. Cho, J.-H.; Azam, A.; Gracias, D.G. Three dimensional nanofabrication using surface forces. *Langmuir* **2010**, *26*, 16534-16539.
79. Puigmartí-Luis, J.; Schaffhauser, D.; Burg, B.R.; Dittrich, P.S. A microfluidic approach for the formation of conductive nanowires and hollow hybrid structures, *Adv. Mater.* **2010**, *22*, 2255-2259.
80. Zheng, W.; Spencer, R.H.; Kiss, L. High throughput assay technologies for ion channel drug discovery. *Assay Drug Dev. Technol.* **2004**, *2*, 543-552.
81. Guan, X.Y.; Gu, L.Q.; Cheley, S.; Braha, O.; Bayley, H. Stochastic sensing of TNT with a genetically engineered pore. *Chem. Bio. Chem.* **2005**, *6*, 1875-1881.
82. Muthukumar, M.; Kong, C.Y. Simulation of polymer translocation through protein channels. *Proc. Natl. Acad. Sci. U.S.A.* **2006**, *103*, 5273-5278.
83. Suzuki, H.; Tabata, K.V.; Noji, H.; Takeuchi, S. Highly reproducible method of planar lipid bilayer reconstitution in polymethyl methacrylate microfluidic chip. *Langmuir* **2006**, *22*, 1937-1942.
84. Malmstadt, N.; Nash, M.A.; Purnell, R.F.; Schmidt, J.J. Automated formation of lipid-bilayer membranes in a microfluidic device. *Nano Lett.* **2006**, *6*, 1961-1965.
85. Poulos, J.L.; Jeon, T.J.; Damoiseaux, R.; Gillespie, E.J.; Bradley, K.A.; Schmidt, J.J. Ion channel and toxin measurement using a high throughput lipid membrane platform. *Biosens. Bioelectron.* **2009**, *24*, 1806-1810.

86. Poulos, J.L.; Nelson, W.C.; Jeon, T.J.; Kim, C.J.; Schmidt, J.J. Electrowetting on dielectric-based microfluidics for integrated lipid bilayer formation and measurement. *Appl. Phys. Lett.* **2009**, *95*, 013706-013709.
87. Lin, C.; Liu, Y.; Yan, H. Designer DNA nanoarchitectures. *Biochemistry* **2009**, *48*, 1663-1674.
88. Sharma, J; Chhabra, R.; Andersen, C.S.; Gothelf, K.V.; Yan, H.; Liu, Y. Toward reliable gold nanoparticle patterning on self-assembled DNA nanoscaffold. *J. Am. Chem. Soc.* **2008**, *130*, 7820-7821.
89. Lee, J.H.; Wernette, D.P.; Yigit, M.V.; Liu, J.; Wang, Z.; Lu, Y. Site-specific control of distances between gold nanoparticles using phosphorothioate anchors on DNA and a short bifunctional molecular fastener. *Angew. Chem. Int. Ed.* **2007**, *46*, 9006-9010.
90. Zheng, J.; Constantinou, P.E.; Micheel, C.; Alivisatos, A.P.; Kiehl, R.A.; Seeman, N.C. Two-dimensional nanoparticle arrays show the organizational power of robust DNA motifs. *Nano Lett.* **2006**, *6*, 1502-1504.
91. Sharma, J.; Chhabra, R.; Cheng, A.; Brownell, J.; Liu, Y.; Yan, H. Control of self-assembly of DNA tubules through integration of gold nanoparticles. *Science* **2009**, *323*, 112-116.
92. Pal, S.; Deng, Z.; Ding, B.; Yan, H.; Liu, Y. DNA-Origami-Directed Self-Assembly of Discrete Silver-Nanoparticle Architectures. *Angew. Chem. Int. Ed.* **2010**, *49*, 2700-2704.
93. Maune, H.T.; Han, S.P.; Barish, R.D.; Bockrath, M.; Goddard, W.A.; Rothemund, P.W.K.; Winfree, E. Self-assembly of carbon nanotubes into two-dimensional geometries using DNA origami templates. *Nat. Nanotechnol.* **2009**, *5*, 61-66.
94. Bolinger, P.-Y.; Stamou, D.; Vogel, H. An integrated self-assembled nanofluidic system for controlled biological chemistries. *Angew Chem. Int. Ed.* **2008**, *120*, 5626-5631.
95. Shim, J.S.; Yun, Y.H.; J Rust, M.J.; Do, J.; Shanov, V.; Schulz, M.J.; Ahn, C.H. Precise self-assembly of individual carbon nanotubes using magnetic capturing and fluidic alignment. *Nanotechnology* **2009**, *20*, 325607.
96. Jaber-Ansari, L.; Hahm, M.G.; Kim, T.H.; Somu, S.; Busnaina, A.; Jung, Y.J. Large scale highly organized single-walled carbon nanotube networks for electrical devices. *Appl. Phys. A* **2009**, *96*, 373-377.
97. Hong, S.W.; Jeong, W.; Ko, H.; Kessler, M.R.; Tsukruk, V.V.; Lin, Z. Directed self-assembly of gradient concentric carbon nanotube rings. *Adv. Funct. Mater.* **2008**, *18*, 2114-2122.
98. Valentini, L.; Bagnis, D.; Kenny, J.M. Organized fluidic assembly of single-walled carbon nanotubes onto fluorine-doped tin-oxide surface with modified wettability. *Carbon* **2008**, *46*, 365-389.
99. Génot, V.; Desportes, S.; Croushore, C.; Lefèvre, J.-P.; Pansu, R.B.; Delaire, J.A.; Rudolf von Rohr, P. Synthesis of organic nanoparticles in a 3D flow focusing microreactor. *Chem. Eng. J.* **2010**, *161*, 234-239.
100. Huang, S.-H.; Tan, W.-H.; Tseng, F.-G.; Takeuchi, S. A monolithically three-dimensional flow-focusing device for formation of single/double emulsions in closed/open microfluidic systems. *J. Micromech. Microeng.* **2006**, *16*, 2336-2344.
101. Shalom, D.; Wootton, R.C.R.; Winkle, R.F.; Cottam, B.F.; Vilar, R.; deMello, A.J.; Wilde, C.P. Synthesis of thiol functionalized gold nanoparticles using a continuous flow microfluidic reactor. *Mater. Lett.* **2007**, *61*, 1146-1150.

102. Zeng, Y.; Harrison, D.J. Self-assembled colloidal arrays as three-dimensional nanofluidic sieves for separation of biomolecules on microchips. *Anal. Chem.* **2007**, *79*, 2289-2295.
103. Seo, Y.H. Nanomesh fluidic filter using self-assembly of colloidal nanospheres and surface tension. *Appl. Phys. Lett.* **2007**, *90*, 123514.
104. Durand, N.F.Y.; Renaud, P. Label-free determination of protein-surface interaction kinetics by ionic conductance inside a nanochannel. *Lab Chip* **2009**, *9*, 319-324.
105. Abgrall, P.; Nguyen, N.T. Nanofluidic devices and their applications. *Anal. Chem.* **2008**, *80*, 2326-2341.
106. Wang, X.; Smirnov, S. Label-free DNA sensor based on surface charge modulated ionic conductance. *ACS Nano* **2009**, *3*, 1004-1010.
107. Lei, Y.; Wang, W.; Wu, W.; Li, Z. Nanofluidic diode in a suspended nanoparticle crystal. *Appl. Phys. Lett.* **2010**, *96*, 263102.
108. Kralchevsky, P.A.; Nagayama, K. Capillary interactions between particles bound to interfaces, liquid films and biomembranes. *Adv. Colloid Interface Sci.* **2000**, *85*, 145-192.
109. Baker, J.L.; Widmer-Cooper, A.; Toney, M.F.; Geissler, P.L.; Alivisatos, A.P. Device-scale perpendicular alignment of colloidal nanorods. *Nano Lett.* **2010**, *10*, 195-201.
110. Wang, M.C.P.; Gates, B.D. Directed assembly of nanowires. *Mater. Today* **2009**, *12*, 34-43.
111. Freer, E.M.; Grachev, O.; Duan, X.; Samuel Martin, S.; Stumbo, D.P. High-yield self-limiting single-nanowire assembly with dielectrophoresis. *Nat. Nanotechnol.* **2010**, *5*, 525-530.
112. Raychaudhuri, S.; Dayeh, S.A.; Wang, D.; Yu, E.T. Precise semiconductor nanowire placement through dielectrophoresis. *Nano Lett.* **2009**, *9*, 2260-2266.
113. Fan, D.L.; Cammarata, R.C.; Chien, C.L. Precision transport and assembling of nanowires in suspension by electric fields. *Appl. Phys. Lett.* **2008**, *92*, 093115.
114. Li, M.; Bhiladvala, R.B.; Morrow, T.; Sioss, J.; Lew, K.-K., Redwing, J.M.; Keating, C.D.; Mayer, T.S. Bottom-up assembly of large-area nanowire resonator arrays. *Nat. Nanotechnol.* **2008**, *3*, 88-92.